The 2024 cascading glacial lake outburst flood in the Thame Valley of Everest region, Nepal: process, impacts and implications

Nitesh Khadka[1], Vishnu Prasad Pandey[1, 2 *], C. Scott Watson[3], Guoxiong Zheng[4, 5], Tianpei Wu[6,7], Keshab Sharma[8], Lauren D. Rawlins[3], Simon Allen[9], Manish Raj Gouli[10], Dibas Shrestha[11]

[1]Center for Water Resources Studies (CWRS), Institute of Engineering, Tribhuvan University, Lalitpur, Nepal
[2]Department of Civil Engineering, Pulchowk Campus, Institute of Engineering, Tribhuvan University, Lalitpur, Nepal
[3]School of Geography and water@leeds, University of Leeds, Leeds, UK
[4]College of Earth and Environmental Sciences, Lanzhou University, Lanzhou, China
[5]Midui Glacier-Guangxie Lake Disaster Field Science Observation and Research Station of Tibet Autonomous Region, Northwest Institute of Eco-Environment and Resources, Chinese Academy of Sciences, Lanzhou, China
[6]State Key Laboratory of Mountain Hazards and Engineering Resilience, Institute of Mountain Hazards and Environment, Chinese Academy of Sciences, Chengdu, China
[7]University of Chinese Academy of Sciences, Beijing, China
[8]BGC Engineering Inc., 330 AlisonBlvd., Fredericton, NB, Canada E3C 0A9
[9]Department of Geography, University of Zurich, Zurich, Switzerland
[10]The Stimson Center - Energy, Water, & Sustainability, 1211 Connecticut Ave, NW / 8th Floor Washington, DC 20036
[11]Central Department of Hydrology and Meteorology, Tribhuvan University, Kathmandu, Nepal

***Correspondence:** Vishnu Prasad Pandey (vishnu.pandey@pcampus.edu.np)

Abstract. On the afternoon of 16 August 2024, a catastrophic flood devastated Thame Village in the Everest region of Nepal. This event resulted from a cascading glacial lake outburst flood (GLOF), where the outburst of an upstream glacial lake triggered the failure of a downstream lake in the headwaters: a complex hazard chain often overlooked in conventional risk assessments. By integrating multi-source satellite imagery, field data, climatic data, empirical estimations, and numerical modelling, we analyse the triggers, processes, and consequences of the cascading failure. We find that the upper lake, which formed in the late 2000s, expanded rapidly to 0.11 km² prior to its outburst, while the lower lake grew by 20% between 1989 and 2024. Our analysis suggests that the moraine-covered bedrock dam of the upper lake was overtopped in response to either (1) a hydrological tipping point driven by intense glacier melt associated with extreme temperatures and precipitation, triggering a cascading failure that ultimately breached the lower lake's moraine dam, or (2) a displacement wave caused by glacier calving or a rock avalanche into the upper lake, causing dam overtopping and initiation of the cascading failure. The event released a combined water volume of approximately 7.7×10^5 m³. Multi-phase mass flow modelling reconstructing two possible scenarios indicates that the flood wave, with an initial peak discharge exceeding 800 m³/s, reached Thame Village within 22 minutes. The socio-economic impact was severe, with losses estimated at 6.18 million USD within the Khumbu Pasang Lhamu Rural Municipality alone, and flood effects traced over 50 km downstream. This event demonstrates that small, rapidly evolving glacial lakes, conditioned by climate-induced glacier retreat, can generate devastatingly powerful GLOFs. This underscores a critical need to broaden GLOF risk assessments to include such small lakes and to prioritize reducing exposure and vulnerability in dynamic high-mountain communities over solely engineering-based hazard control.

Keywords: cascading GLOF, climate change, disaster risk reduction, multi-phase mass flow, Thame Valley

1 Introduction

Glacial Lake Outburst Floods (GLOFs) are high-magnitude events in mountainous regions that can evolve into hyper-concentrated or debris flows, leading to substantial hydrological, geomorphological, and socio-economic impacts downstream (Cook et al., 2018; Veh et al., 2020; Sattar et al., 2025b). A total of 569 reported GLOF events have been documented over High Mountain Asia (HMA) up to 2022 (Lützow et al., 2023). Across HMA, the risk of GLOF is expected to increase in future by three-fold amidst ongoing climate change induced glacial recession and evolution of glacial lakes (Zheng et al., 2021b). Thus, risk assessment of present glacial lakes (Zhang et al., 2023c) and modelling future lake formation and predicting their GLOF hazard (Furian et al., 2021; Zheng et al., 2021b; Furian and Sauter, 2025) are essential for the early identification of GLOF risk hotspots. Current regional scale (Allen et al., 2019; Zhang et al., 2022), national scale (Rounce et al., 2017; Dubey and Goyal, 2020; Chen et al., 2025) to case specific GLOF risk assessments and field studies (Sattar et al., 2021; Allen et al., 2022; Rinzin et al., 2023; Gouli et al., 2025) in the Himalayan region are mainly targeted at glacial lakes of considerable size, often neglecting small glacial lakes owing to their low potential flood volume. However, global assessment shows the dominance of outburst floods from small glacial lakes (Veh et al., 2025). Additionally, GLOF events in the Himalaya such as 2013 Kedarnath disaster in India (Allen et al., 2016), 2016 Gonbatongshaco GLOF along the China-Nepal border (Sattar et al., 2022; Chen et al., 2023) and 2017 Langmale GLOF (Byers et al., 2018) have shown that even small lakes can cause devastation downstream.

On 16th August 2024 at 1.30 pm, Thame Village in the Everest region of Nepal experienced a sudden and extreme flooding event, prompting authorities to issue alerts for the downstream region. The following day, a helicopter survey by Government of Nepal revealed that this flooding was triggered by a cascading outburst of two glacial lakes located in the headwaters of Thame Valley (Ghimire, 2024). These lakes were relatively small in size (<0.1 km^2) compared to nearby glacial lakes such as Tsho Rolpa (1.67 km^2 in 2022) and Imja Tsho (1.73 km^2 in 2022) which have been studied in detail (ICIMOD, 2011; Khadka et al., 2019) and also have undergone GLOF remediation works (Cuellar and McKinney, 2017; Lala et al., 2018). Due to their relatively small size, these lakes were missed in the previous GLOF hazard and risk assessments at regional and local scales (Table 1). Among previous studies, Zhang et al. (2023c) included these glacial lakes in their comprehensive GLOF risk assessments in HMA and reported one lake (upper lake 1, Fig. 1) to have high GLOF hazard. This highlights limitations of existing GLOF hazard assessments (Table 1), particularly the use of minimum lake-size thresholds for screening glacial lakes and the limited consideration of cascading outburst processes, whereby failure of an upstream lake can trigger downstream lake breaches. Site-specific investigation of GLOFs and the dissemination of information, including their occurrence dates, triggers, process and impacts, is essential for understanding the nature and behaviour of outburst floods, particularly in the context of climate change (Westoby et al., 2014; Mergili et al., 2018a; Nie et al., 2020). Several studies have explored the evolution, triggers and reconstructed the past history of GLOF events. For example, 2001 Chongbaxiaco GLOF in eastern Himalaya (Nie et al., 2020), 2014 Gya GLOF in Indian Himalaya (Majeed et al., 2021), 2018 Langmale GLOF in Nepal (Byers et al., 2018), 2002 and 2016 GLOFs in Poiqu river basin, central Himalaya (Wang et al., 2024), 2020 Jinwuco GLOF in Tibet (Zheng et al., 2021a), 2023 South Lhonak GLOF (Sattar et al., 2025b; Zhang et al., 2025) and 2024 Birendra lake GLOF (Khadka et al., 2024b; Poudel et al., 2025) were analysed and reconstructed. Collectively, these studies not only provide insights into the mechanisms and triggers of GLOFs, but also contribute to the enhancement of future GLOF risk assessment frameworks, better develop GLOF models, and aid in effective disaster risk reduction and mitigation strategies.

The outburst of lower Ngole glacial lake was due to an overtopping from the upper Ngole glacial lake. When multiple lakes are arranged in series within a watershed, the overtopping or failure of an upstream lake may trigger a cascading GLOFs from downstream lakes, generating a "domino effect" that substantially amplifies flood magnitude and destructive potential through flow bulking. This GLOF occurred during the monsoon season (June to September), a period characterized by elevated temperatures, significant precipitation, and increased river discharge (Salerno et al., 2015; Sharma et al., 2020). The cascading GLOF resulted in severe damage to Thame Village, trekking trails and several infrastructures in the Everest region. Although previous reports have examined the possible triggers and impacts of the 2024 Thame GLOF (Maharjan et al., 2025; Munch et al., 2026), they lacked a comprehensive analysis integrating precise drained water volume estimation and cascading GLOF reconstruction. Thus, in this study, we aim to (i) track the long-term evolution of these two glacial lakes using satellite observations, (ii) identify the possible triggers, (iii) analyse the conditioning factors that led to the trigger, (iv) reconstruct the cascading GLOF process chain using numerical modelling, and (v) report the downstream impacts of the GLOF. Further, we assess and discuss the potential future GLOF hazard from these lakes and outline several strategies for GLOF risk reduction in the area. Finally, this study will contribute to better understanding of the cascading Thame GLOF process chain and underscores the need to reconsider the prioritization of small glacial lakes in future GLOF risk assessment and disaster risk management in the high Himalayan regions.

Table 1. List of studies that have identified dangerous glacial lakes including the Everest region of Nepal.

Study	Study area	Method	Minimum lake size (km^2)
ICIMOD (2011)	Nepal	Qualitative	>0.2
Rounce et al. (2017)	Nepal	Quantitative and decision-based classification	≥0.1
Bajracharya et al. (2020)	Nepal and transboundary areas	Qualitative	≥0.2
Khadka et al. (2021)	Mahalangur Himal	Quantitative: Weight based multi-criteria	≥0.05
Zheng et al. (2021b)	HMA	Quantitative with equal weights	≥0.05
Hu et al. (2022)	Nepal	Quantitative: Weight based multi-criteria	≥0.2
Zhang et al. (2023c)	HMA	Quantitative: Weight based multi-criteria	≥0.01

2 Study area

The present GLOF site is located in the Thame Valley of Dudh Koshi basin of eastern Nepal Himalaya, often also referred as Everest region or Khumbu Himal (Figure 1) (Byers, 2017). Nepal Himalaya hosts a dense distribution of glaciers and glacial lakes in the northern part of the country (Khadka et al., 2023). In response to climatic warming, glaciers in Nepal have shrunk by 14% between 1970 and 2010 (Khadka et al., 2023) whereas the surface area of glacial lakes have undergone 25% expansion between 1987 and 2017 (Khadka et al., 2018). The climate of this region is affected by the South Asian monsoon in summer and by westerlies in winter (Salerno et al., 2015). Most glaciers in the Everest region are valley type with expansive debris cover in the ablation zone (Thakuri et al., 2014). Nine large glaciers in the region exhibited a negative mass balance of –0.52 ± 0.22 m water equivalent (w.e.) a^{-1} during 2000–2015 (King et al., 2017). Among different regions of Nepal, the expansion rate of glacial lakes is reported to be the highest (1.37 km^2 per decade) in the Everest region (Khadka et al., 2018). This region has also witnessed at least nine GLOF events (Figure 1b), among which the 1985 Dig Tsho GLOF (Vuichard and Zimmermann, 1987) and the 1998 Tam Pokhari GLOF (Lamsal et al., 2016) caused notable downstream socio-economic impacts.

The Thame Valley lies in the east of Sagarmatha National Park under Khumbu Pashung Lamu Rural Municipality (KPL RM) Ward Number 5 and had a population of 1255 in 2021 (National Statistic Office, 2023). At an elevation of 3,800 m (above sea level), Thame Village is located ~5 km from Namche bazar, a large settlement and key touristic gateway to Mt. Everest. Positioned enroute to Thashi Lepha pass and Renjo La pass, Thame attracts many trekkers and tourists, with the village hosting numerous houses, lodges and restaurants, a health post and school, Buddhist Monastery, and a small hydroelectric power plant (930 kW). The headwaters of the valley are home to seven glacial lakes, five of which are clustered in close proximity to one another (Fig. 1c). The upper Ngole glacial lake (4,890 m a.s.l) is the initial source of flood, which experienced a breach that triggered an outburst from the lower glacial lake, known as Ngole Pokhari (where "Pokhari" meaning "pond" in Nepali), leading to a cascading GLOF. The upper Ngole lake is situated at the terminus of a debris-covered glacier (G086552E27827N) with a catchment area of ~5 km^2, and is dammed by bedrock, overlaid with glacial moraine. The lower Ngole glacial lake (4,718 m a.s.l) is a moraine-dammed lake with a catchment area of ~9 km^2, located approximately 700 m below the upper lake and is part of the same glacier that has retreated since the end of the Little Ice Age and now no longer exists (Fig. S1) (Lee et al., 2021). The moraine dam of lower lake is composed of a diverse and well-graded mixture of silt, sand, gravel, cobbles, and boulders, with some clast sizes reaching or even exceeding 5 m in diameter (Figure 2).

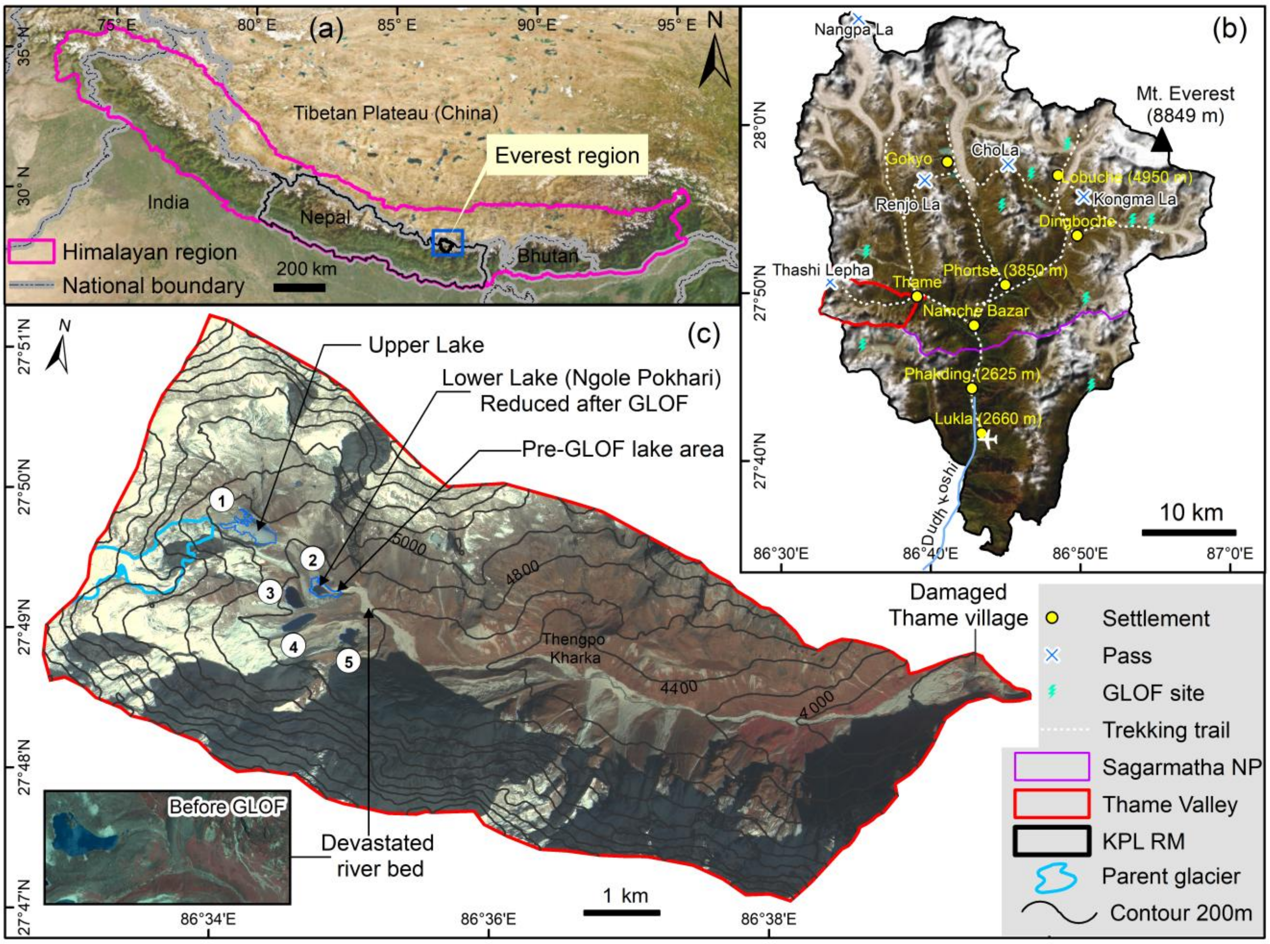

Figure 1: Study area showing the location of GLOF site. Study area in the border regional level (a) and at Khumbu Pasang Lamu Rural Municipality (KPL RM) of Nepal (b) with enlarged Thame Valley showing the topography after the GLOF event (c). The base images (a and b) are produced by ESRI (Sources: Esri, TomTom, FAO, USGS | Powered by Esri) and a Gaofen image of August 18, 2024 (c). The figure was created by authors using ArcGIS® software by Esri.

3 Materials and Methods

We employed a variety of data sources for this study, including multi-source optical remote sensing data, digital elevation models (DEM), reanalysis and station-based climate data, field measurements, and additional auxiliary datasets. A summary of these datasets is presented in Table 2, while the subsequent sections detail their specific applications in the study.

Table 2. Datasets used in this study for various purposes.

No.	Data	Acquisition date	Repeat cycle (days)	Spatial resolution (m)	Purpose
1	Landsat MSS*	1976-11-13	16	60	Lake mapping
2	Landsat-5 TM*	1989-11-09; 1995-10-09; 2000-11-23; 2010-12-05	16	30	Lake mapping
3	Landsat-8 OLI*	2015-11-17	16	30	Lake mapping
4	Sentinel-2	2020-10-09; 2022-05-17; 2024-11-27; 2025-03-29	5	10	Lake mapping
5	Planet Scope	2024-08-15; 2024-08-16	1	3	Lake mapping, and cause analysis of GLOF
6	Gaofen-2/7	2024-05-30; 2024-08-18; 2024-10-31	Gaofen-2: 16 Gaofen-7: 12	1-0.65	Lake mapping, cause and impact analysis of GLOF
7	HMA-DEM	2014-2016 mosaic (MO_20170716_tile-677)	-	8	Topographic analysis and GLOF process chain
8	ERA5 Land (reanalysis data)	1990-2024	hourly	9 km	Climatological study and cause analysis
9	Meteorological station data	2019-2024	hourly	daily	Climatological study (support to reanalysis data)
10	Composite Ice thickness (raster data)	2020	-	-	Estimate the height of icebergs
11	Drone-derived DEM	24 May 2025	-	-	Estimated the drained volume of both glacial lakes

*MSS- Multi-spectral Scanner; TM-Thematic Mapper; OLI-Operational Land Imager

3.1 Delineation of glaciers and glacial lakes

We used multi-source optical remote sensing datasets (Table 2) to track the area of glacier and glacial lakes from 1976 to 2024. Glacier and glacial lake outlines were manually delineated from the geometrically corrected false colour composite images (NIR/red/green) of satellite data by a single expert (Wang et al., 2020). The error associated with the delineation of individual lake boundaries was calculated as the product of half the image resolution and the lake's perimeter. This error calculation is predicted on the assumption that, on average, the lake margin intersects the centres of the pixels along its perimeter (Salerno et al., 2012).

3.2 Field-based and empirical quantification of the event and cause analysis

During field investigation (Nov-Dec 2024), we engaged with local residents of Thame Village, stakeholders and rural municipality to gather insights on the timing and impacts of this event through interview and informal discussions. These consultations provided qualitative information on the timing and progression of the flood, observed impacts, and community experiences before, during and immediately after the GLOF. We explored the potential causes of this GLOF and employed a Global Navigation Satellite System (GNSS) to measure the lowering of the lake levels after their outbursts.

We utilized a laser range finder to assess the width and depth of the breach in the moraine dam of the glacial lakes (Figure 2), as well as changes in the river morphology and geomorphology in Thame Village. Additionally, the breach parameters for upper lake were also obtained and verified from the field report of International Centre for Integrated Mountain Development (ICIMOD) (Maharjan et al., 2025).

A high-resolution (1 m) DEM was acquired via uncrewed aerial vehicle (UAV) surveys on 24 May 2026. The drainage volume of the upper and lower lakes was reconstructed using the lake outlines and the drone-derived DEM. The post-GLOF lake water surface elevation was estimated by sampling elevations along the lake perimeter from the DEM and assigning the median elevation to all cells within the post-GLOF lake outline, thereby creating a flat-water surface. The pre-GLOF lake surface was reconstructed using the same approach. The reconstructed pre- and post-GLOF water surfaces were differenced, and the resulting elevation differences were multiplied by the grid-cell area and summed to estimate the drained lake volume. For this, lake outline delineated before (2024-08-15) and after (2024-08-18) the event was utilized. The water volumes of upper and lower lakes were empirically estimated using average of nine area-volume relationships (see Tables 3 and S1). Further, the obtained drained volumes from drone-derived DEM were also compared with empirically estimated drained volume (refer Text S1 and Table S1).

The peak discharge during the GLOF event and the timing of the dam breach formation were also derived empirically based on the released volume and lake lowering height. The released volume was calculated as described above based on drone-derived DEM, while the lake lowering height and breach dimensions were determined through field measurements (Figure 2). Various empirical equations commonly found in the literature were utilized for estimation purposes, and the overall average of these calculations was taken as the final estimate for both peak discharge and the timing of breach formation (Tables 3 and S2). The total volume released, peak discharge, and timing of the dam breach for the cascading event were analysed by combining the released volumes from both the upper and lower lakes (Tables S1 and S2).

The different possible triggering factors of the GLOF were analysed based on field observations, published news/reports and through examination of fine-resolution remote sensing images (See Section 4.2). Icebergs were manually delineated from PlanetScope (3 m) and Gaofen-7 images (0.65 m) of 2024-8-15/16 and 2024-08-18, respectively. The icebergs, both pre- and post-GLOF, as well as those that are grounded and drifting, were identified through a comparative analysis of the images (Fig. S2). The volume of icebergs was determined based on the area-volume relationship as shown in Equation 1. This equation was derived by Watson et al. (2020) through detailed study of calving and iceberg formation of Thulagi glacial lake in Nepal.

$$V_i = 4.3017A^{1.19} \quad \ldots \ldots \qquad (1)$$

Where, V_i is volume of icebergs in m^3 and A is surface area of icebergs in m^2.

Table 3. Studies whose empirical equations were used to calculate three parameters. The details of the equations and the calculations are given in supplementary Tables S1 and S2.

Parameter calculated	Studies whose empirical equations were used
Lake Volume (V)	Evans (1986); Huggel et al. (2002); Wang et al. (2012); Sakai (2012);Khanal et al. (2015) ; Cook and Quincey (2015);Kapitsa et al. (2017) ; Zhang et al. (2023a); Zhang et al. (2023b)
Peak discharge	Evans (1986); Popov (1991); COSTA and SCHUSTER (1988); Costa (1985); Costa (1985); Froehlich (1995); Froehlich (2025)

Breach time	Froehlich (1995); Froehlich (2025)

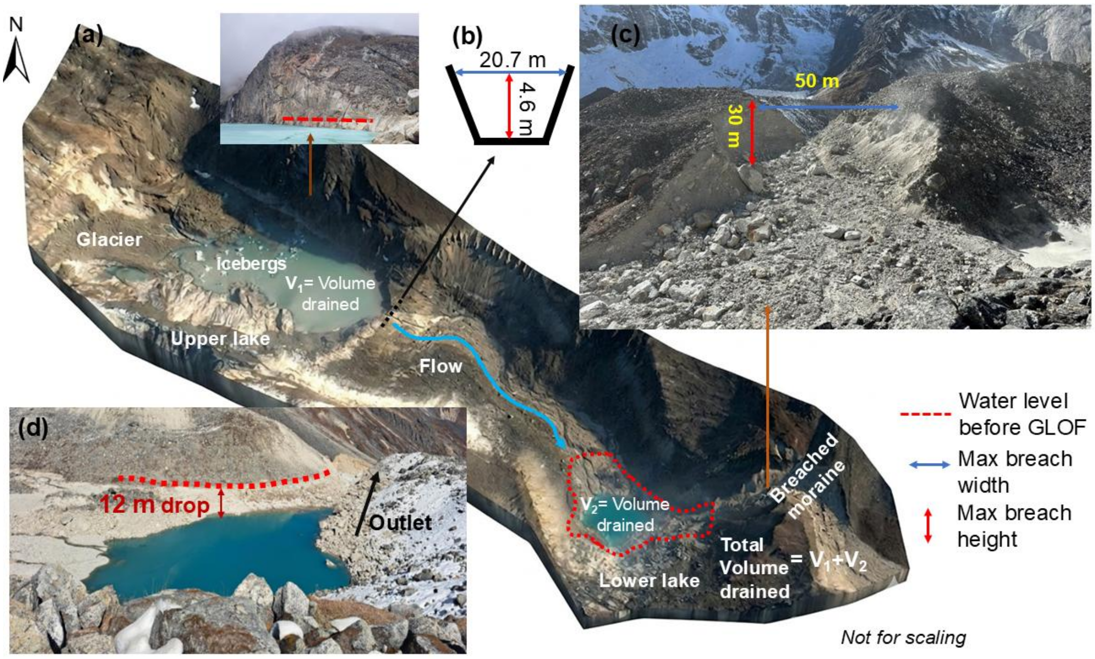

Figure 2: Images showing the breach mechanism and associated breach parameters following the cascading GLOF. (a) The outburst of upper lake cascades into lower lake, resulting its outburst, which is characterized by a reduced water level and a breached terminal moraine. (b) Breach parameters of the upper lake and (c) lower lake and (d) observed decrease in water level of the lower lake. The image in (a) is from Gaofen-7 satellite while those in (c) and (d) are obtained from field.

3.3 Climatic analysis

We used ERA-5 Land data, the global reanalysis dataset which provides long-term data on climate variables since 1950 (Muñoz-Sabater et al., 2021) and has good performance in the Nepal Himalaya (Chen et al., 2021). ERA5-Land dataset aggregated at daily timestep was accessed using the Google Earth Engine (GEE) platform. Daily aggregates in GEE are pre-calculated daily from hourly values. We extracted the daily aggregated 2-m air temperature (24-hour average) and precipitation (24-hour total) for the lake area from 1990 to 2024. The days with extreme temperature and precipitation exceeding 90^{th} and 95^{th} percentiles were calculated with respect to long-term time series (1990–2024) data. Additionally, data from the Phortse Automatic Weather Station, located 11 km east of Thame Village at the same elevation (3,850 m), was utilized to obtain observed values of temperature and precipitation for the area.

3.4 Cascading GLOF simulation with r.avaflow

Cascading GLOF processes were simulated using r.avaflow (v. 4.0G), an open-source multi-phase computational tool for complex mass flow dynamics in mountain regions (Mergili and Pudasaini, 2014-2025). Unlike traditional single-phase models, r.avaflow employs a coupled multi-phase approach to accurately characterize phase interactions and material entrainment, enhancing the simulation of cascading hazards (Mergili et al., 2017). Its core algorithm, developed by Pudasaini and Mergili (2019), propagates mass flow across a DEM using depth-averaged continuity and momentum equations (Mergili et al., 2018b). The model employs a second-order TVD-NOC (Total Variation Diminishing Non-Oscillatory Central Differencing) scheme on a staggered grid for spatial discretization, ensuring both accuracy and stability (Tai et al., 2002). Operating with GIS raster cells, it facilitates mass-flow exchanges between adjacent cells at each time step (Mergili et al., 2025). Integrated within GRASS GIS 7, r.avaflow combines Python/C code with R-based statistical tools for efficient simulation and analysis, as detailed by Mergili et al. (2017).

We modelled the cascading GLOF process chain based on two scenarios that encapsulate the extremes of potential mechanisms within the event. In Scenario A, we assumed a rapid inflow generated by the upstream lake breach entered the downstream lake and produced displacement wave that overtopped the dam crest and progressively eroded the moraine dam. However, in Scenario B, the inflow from the upstream lake was assumed to gradually increase the water level (and storage volume) of the downstream lake until it reached the dam crest, subsequently resulting in dam failure.

For GLOF simulation, the volume of the lake, peak discharge, and breach timing were empirically estimated (Sections 3.2 and 4.2), while other dam and breach parameters were sourced from field measurements (Figure 2). For both scenarios, lower lake volume modelling was performed using r.lakefill function, a GRASS GIS script used within the r.avaflow and HMA DEM. Following previous moraine dam GLOF studies, the value of the lake dam entrainment coefficient was taken as $10^{-5.7}$ (Zhang et al., 2025). In Scenario A, an idealized triangular hydrograph (Huggel et al., 2002; Froehlich, 2025) was developed based on upper lake estimates of drained volume and peak discharge for input into the lower lake (see Fig. S3). For Scenario B, a GIS-based analysis was conducted, revealing that the drained upstream lake volume resulted in 11.8 m rise in water level prior that exceeded the dam crest leading to the dam's failure.

Other essential input parameters for the simulations in both scenarios are summarized in Table 4 which were mainly derived from existing studies (Mergili et al., 2020b; Rinzin et al., 2025; Zhang et al., 2025; Chen et al., 2026) and obtained through optimization at the early stage of simulation. The selected parameter set yielded good agreement with the observed flood extent and flow routing, resulting in satisfactory accuracy assessment scores (see Section 4.4). The HMA-DEM (Table 2) was utilized to represent the terrain owing to its greater resolution and all simulations were executed with a cell size of 10 m. The total simulation duration was set to 3,600 seconds (1 hr). The analysis was confined to Thame Village, which is approximately 9 km downstream from the upper lake, as this area experienced the most significant damage. This limitation was necessitated by the unavailability of HMA-DEM data further downstream, as well as to reduce uncertainties associated with the complex topography of the Himalayan region.

The accuracy assessment of GLOF reconstruction was conducted by comparing the satellite-derived inundation area with the modelled flood extent. An overlay analysis was performed to calculate true positive, false positive, and false negative areas (see Text S2). From these, precision and recall were computed, followed by the F1 Score to provide a balanced measure of overall inundation accuracy (Text S2). These metrics yield a score between 0 and 1, with 1 indicating a perfect alignment between the two datasets being compared (Rawlins et al., 2026).

Table 4 Basic input parameters used for r.avaflow simulation.

Parameter	Unit	Value
Cell size	m	10
Density of solid phase (ρ_s)	kg/m³	2,700
Density of fluid phase (ρ_f)	kg/m³	1,000
Simulation time (T)	s	3,600
Internal friction angle (Φ)	°	25
Basal friction angle (δ)	°	15
Fluid friction number	-	0.05

3.5 Impacts of the GLOF

The impact assessment of the GLOF was conducted by synthesizing the detailed flood incident report on losses and damages compiled by the local government i.e., KPL RM (https://khumbupasanglhamumun.gov.np/). Furthermore, additional impacts were gathered from a field study, and news and institutional reports. Reported damage to trekking trails in the Thame Valley was cross-verified using high-resolution GaoFen-2/7 satellite imagery by comparing the reported length of damaged trails with the length of visible post-event damage observed in the imagery.

4 Results

4.1 Evolution of glacial lakes

The evolution of the glacial lake cluster located in the headwaters of Thame Valley is shown in Fig. 3. The upper Ngole lake (Lake 1) started to form in the beginning of the 21st century with progression of its parent glacier shrinkage (Fig. 4a) and reached a considerable size of 0.018 ± 0.009 km^2 in 2010 (Figs. 3b and 4b). With rapid expansion in recent years (Fig. S4), it reached an area of 0.11 ± 0.004 km^2 before its outburst. After its outburst, the area slightly reduced by 0.013 km^2.

The lower Ngole lake (Lake 2) started to evolve before the 1980s, with an area of 0.04 ± 0.01 km^2 in 1989. It grew by 20% in the last 35 years (Fig. 4b). The area reduced from 0.048 ± 0.01 km^2 to 0.015 km^2 after its outburst in August 16, 2024. The other lakes (lakes 3 and 4) on the southern sides were present from 1989 and a slight fluctuation of ± 0.01 km^2 is observed between the years (Table S3). Lake 5 is transient in nature and is mostly observed in monsoon season when snow-glacier melt and rainfall are common (Fig. S4). The areas of lakes 3, 4 and 5 are 0.042, 0.042 and 0.01 km^2, respectively as derived from a Gaofen-7 image of 2024-08-18.

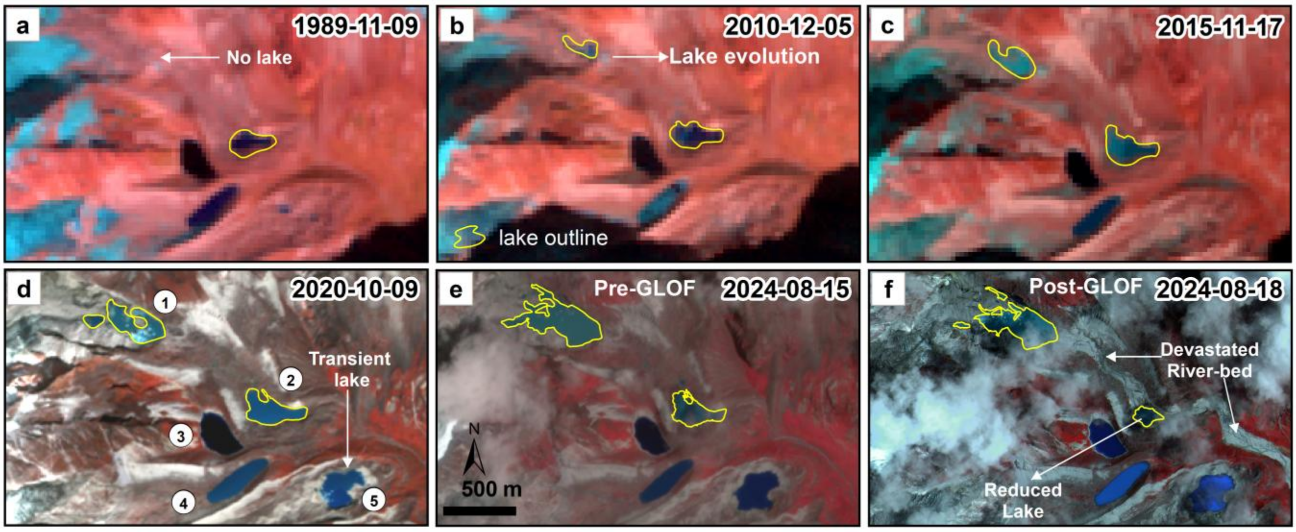

Figure 3: The evolution of glacial lakes located in the headwaters of Thame Valley in the Everest region. The background images are from Landsat (a, b and c), PlanetScope (d and e) and Gaofen (f) satellites. The figure was created by authors using ArcGIS® software by Esri.

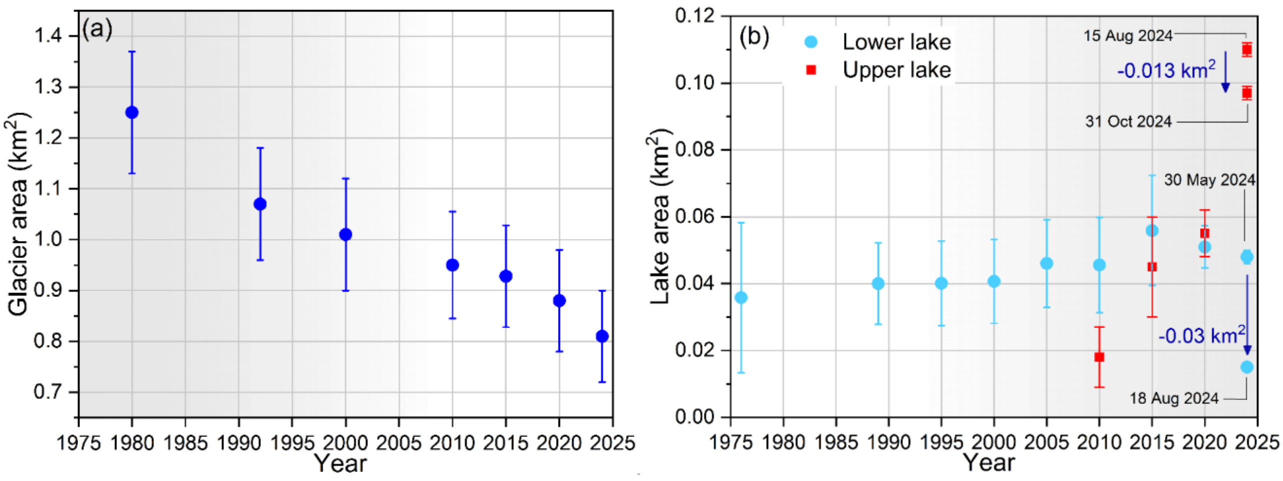

Figure 4: Changes in the area of the parent glacier (a) and the upper and lower Ngole glacial lakes (b) from 1976 to 2024.

4.2 Potential triggers and quantification of the event

Analysing the various potential triggering and conditioning factors (Table 5), it becomes evident that the likely cause for the outburst of the upper glacial lake is potentially linked to extreme temperature-induced snow and glacier melt, coupled with calving from the parent glacier (debris-covered). These processes would increase the lake's water volume, which potentially initiated a dam failure of the thin moraine dam (~3-4 m thick), which overlaid bedrock (Figure 5). However, the highly fragmented rock slopes along the eastern margin of the upper lake suggest that rock avalanches may have occurred (see Section 5.2), potentially generating displacement waves that overtopped the dam and triggered the GLOF. The displacement wave mechanism, irrespective of the potential trigger, is represented by Scenario A in our modelling.

The total surface areas of the delineated drifting icebergs (>130 m^2) in upper lake before the GLOF were 3,117 ± 1,413 m^2 with corresponding volume of 61,905 ± 24,145 m^3 (Figure 5 and S2). We estimate icebergs to have a total height of ~15-25 m, based on composite ice thickness raster data (Table 2) with more than 80 % to be considered submerged underwater. The glacier melting and calving events are linked to the extreme air temperatures (see Section 4.3). Our estimate from drone-derived DEM calculations indicates that approximately 4.1 × 10^5 m^3 of water drained from the upper glacial lake. The lake level lowered by approximately 4.6 m and dam breached by approximately 21 m (Figure 2b). The total surface areas of the drifting ice-bergs (>20 m^2) after its outburst were 7,092 ± 1,210 m^2 with a volume of 162,921 ± 19,982 m^3 (Figure 5d and S2).

The subsequent outburst flood from the upper glacial lake triggered the GLOF from lower glacial lake. The floodwaters from the upper lake descended approximately 182 m and travelled about 700 m before plunging into the lower lake (Fig. S1). The steepest section is immediately adjacent to the upper lake, where the bedrock step drops 100 m vertically over a 120 m horizontal distance. The rapid influx of water and sediment substantially increased the volume of lower lake and generated surge waves in lake surface water that ultimately led to the failure of the moraine dam. Our estimate indicates that approximately 3.6 × 10^5 m^3 of water drained from the lower glacial lake. Subsequently, the lake level has lowered by approximately 12 m and dam has incised by approximately 50 m (Figure 2).

A total of approximately 7.7 ×10^5 m^3 of water was released from both lakes during the event. The drone-derived DEM and empirical methods yielded broadly comparable estimates of total drained volume, differing by 28.3 % (Text S1). The lower lake estimates were in close agreement (2.9 % difference), whereas the upper lake showed a larger discrepancy (64 %).

Interviews with local residents indicated that the days preceding the GLOF were perceived as unusually warm. Although the reported timings varied among respondents, residents consistently stated that the flood occurred during the afternoon of 16 August 2024. Records from local authorities and other stakeholders indicate that the flood reached Thame Village at approximately 13:30 local time. A Planet satellite image acquired at around 10:00 local time on the same day showed no evidence of an outburst at the source area (Fig. 5). Together with the reconstructed flood travel time of approximately 20-25 minutes from the source lakes to Thame Village (Section 4.4), these observations suggest that the GLOF was initiated at around 13:00 local time.

Table 5. Analysis of different conditioning and triggering factors of the cascading GLOF.

Conditioning and triggering factors analysed	Upper lake	Lower lake	Analysis and remarks
Ice-snow avalanche	Not evident	Not applicable	Immediate field observations by government institutions and Sagarmatha Pollution Control Committee
Rockfall or landslides	Evident*	Not applicable	Field observation shows the deposits of probable rock avalanches on the north-east zone from the fragmented steep rocky terrain; however, these appear weathered and old. Further, according to locals and satellite images, the rockfall deposits were there long before the GLOF (Fig. S5). Additionally, high-resolution Gaofen-7 imagery (0.65 m) and visible geology shows no clear signs of rock fall immediately prior to the GLOF (Fig. 4). However, this is limited by the resolution of the imagery.
Calving of glacier or glacier retreat	Evident	Not applicable	Evidence of a wide calving front, large and numerous ice-bergs visible on Planet and Gaofen-7 satellite images
Lake size/volume increment	Evident	Not evident	Analysis of multi-source remote sensing images
Dead ice melting	No dead ice present	No dead ice present	Field and satellite image observation
Prior days with extreme temperature	Evident	Evident	Analysis of ERA5-Land datasets and interview with locals
Prior days with extreme precipitation	Evident	Evident	Evident from analysis of ERA-5 Land data
Seismicity	Not evident	Not evident	Not recorded
Permafrost degradation at dam sites	Not evident	Not evident	Not expected below 5000 m according to Singh et al. (2025)
Upper lake outburst	Not evident	Evident	Remote sensing analysis

*As reported by previous study (Maharjan et al., 2025).

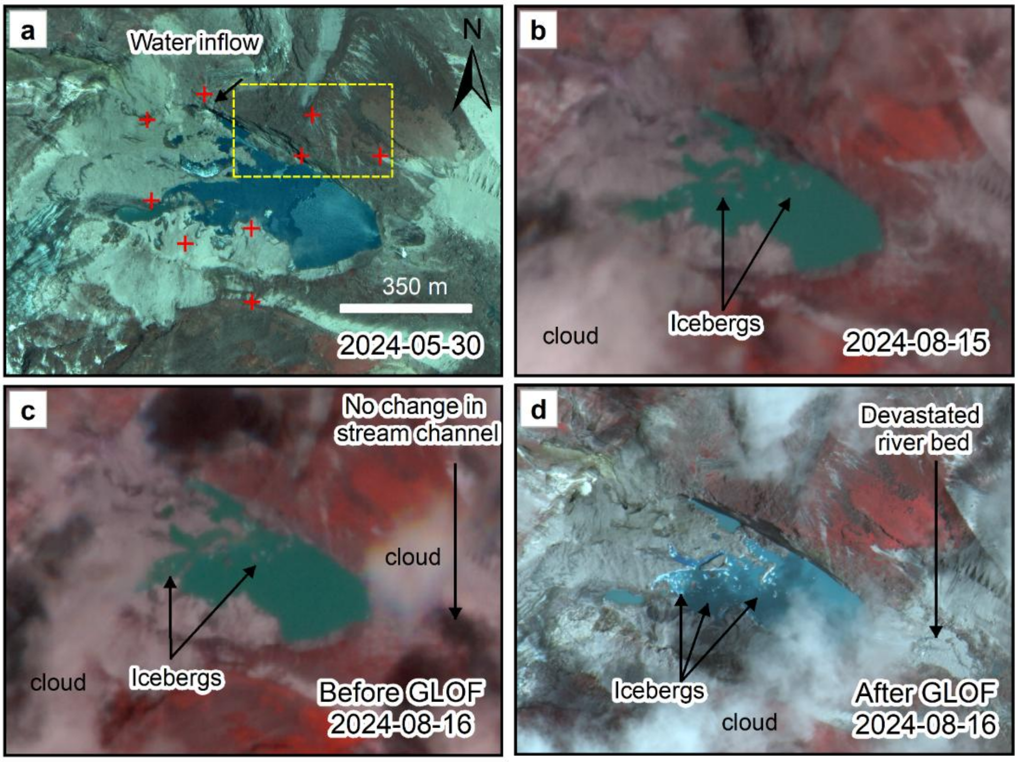

Figure 5: Monitoring changes in upper lake and surroundings before and after the GLOF. The red plus points indicate control points used for monitoring the changes in land surface. The yellow dashed box shows a zone of rockfall with no visible change. The image (c) is sensed on the same day just prior to the GLOF, reveals no sign of mass movement into the lake but formation of icebergs due to calving. Further, there does not appear to be any noticeable increase in the upper lake's turbidity in the post-GLOF image, e.g. caused by a rockfall. Background images (a) and (d) are sourced from Gaofen-2/7, whereas (b) and (d) are from PlanetScope. The figure was created by authors using ArcGIS® software by Esri.

4.3 Meteorological analysis

In the month leading up to the occurrence of the GLOF, several days experienced temperatures and precipitation levels that exceeded the 90th and 95th percentiles thresholds derived from long-term (1990–2024) daily climatology (Fig. 6). During summer months (JJAS), climatic conditions are generally warmer and wetter than during preceding spring season (MAM) in Nepal. Specifically, the temperatures on 12–15 August, immediately prior to the GLOF event on August 16, surpassed both the 90th and 95th percentile thresholds. Likewise, the precipitation on August 14 and 15 also exceeded both 90th and 95th percentiles (Fig. 6a and b). Similarly, the exceedances in temperatures and precipitation were observed during July. Compared with the same 30-day period during 1990–2024, the pre-event period (17 July–15 August 2024) was the warmest on record, with temperature exceeding the both 90th and 95th percentile thresholds (Fig. S6a).

The average annual temperature and the maximum monthly temperature during the summer seasons in the Ngole lake region have been observed to be increasing at rates of 0.015 °C and 0.003 °C per year, respectively, between 1990 and 2014 (Fig. 6d). On the day preceding the outburst, the ERA5-Land data recorded minimum and maximum temperatures of 3.7 °C and 9.7 °C, respectively with consecutive extreme wet days exceeding 10 days (Fig. 6c). Concurrently, data collected from the Phortse automatic weather station, located 11 km east at an elevation of 3,850 m, reported minimum and maximum temperatures of 7.45 °C and 14.13 °C, respectively, along with a total rainfall of 124 mm over a consecutive 14-days wet period prior to the GLOF event (Fig. S6b). This implies that the data of ERA5-Land, though being reanalysis, captures the general climatic conditions and trends of the region (Chen et al., 2021). These climatic conditions are conducive to increased glacier and snow melt, which might have been contributed glacier melt and calving, and initiation of the GLOF.

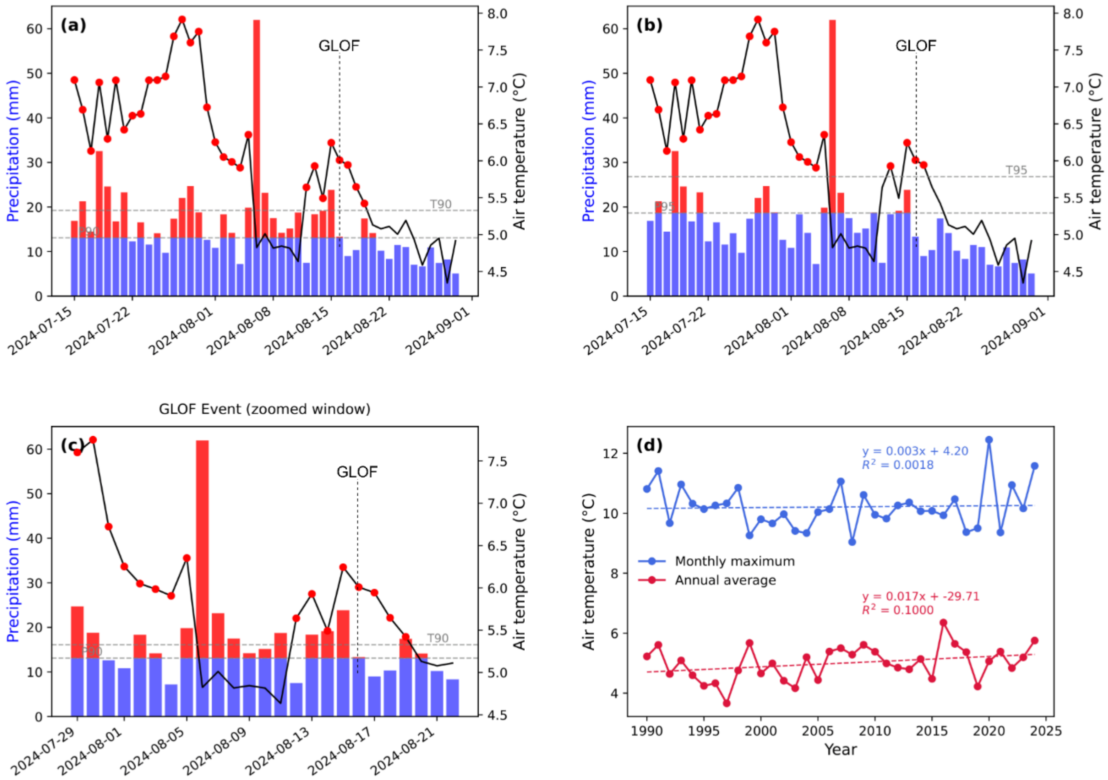

Fig. 6: Meteorological conditions of the lake region. (a) Extreme air temperature and precipitation values (red colour) before the GLOF event exceeding the 90th percentile (a) and 95th percentile (b) compared to long term (1990-2024) average climatology, a zoomed view (c) for enhanced reading and (d) the trends of annual average temperature and maximum monthly temperature of that year from 1990 to 2024.

4.4 Cascading GLOF reconstruction

The reconstructed GLOF flow heights, arrival times, hydrographs and velocity for both scenarios A and B are shown in Figs. 7, 8, 9 and S7. Accuracy assessment of reconstructed GLOF inundation areas show that Scenario A achieved precision, recall, and F1 scores of 0.73, 0.85, and 0.78, respectively, while Scenario B yielded 0.71, 0.83, and 0.77. Overall, these metrics indicate acceptable model performance in capturing the actual flood extent, with Scenario A being marginally more accurate than Scenario B.

In Scenario A, the simulation results reveal the dynamic characteristics of the event and its downstream impacts. The inflow hydrograph of the upstream lake (Fig. S3) exhibits a sharp peak of approximately 586 m³/s within 699 s. This surge wave with velocities 15 m/s, released from Input1, first impacted the downstream lake, initiating its breach and generating a compound flood. At the immediate downstream outlet (O1), the discharge hydrograph displays peak exceeding 800 m³/s and lasting for more than 2000 s, reflecting a complex breach evolution process (Figure 9a). At 800 s after the breach, the liquid-phase discharge at O1 reached a peak of 912 m³/s, accompanied by the release of solid-phase material derived from the erosion of the dam body during failure. The combined flood wave then propagated downstream, reaching Thame Village (O2) 1300 s (approximately 22 min, Figure 8) after the initial breach with maximum discharge of 574 m^3/s, maximum flow heights up to 4 m and velocity of 10 m/s (Figure 7, 9 and S7). Although significant channel storage effects and energy dissipation reduced the peak discharge at O2 to approximately 548 m³/s, the magnitude and duration of the flood remained sufficient with depositions to cause severe damage, highlighting the long-term hazard posed by cascading GLOF events.

In Scenario B, in contrast to the sudden displacement wave in Scenario A, the failure was induced by sustained inflow from the upstream lake, which progressively increased the storage and water level of the downstream lake until overtopping and structural collapse occurred. The hydrographs illustrate the dynamic features of this breach mode. The discharge at O1 (breach output 1) shows a rapid rise to multiple peak flow, a characteristic feature of dam-break floods, followed by gradual recession (Figure 9b). At 240 s after the breach, the liquid-phase discharge at O1 reached a peak of 1,240 m^3/s, accompanied by the outflow of solid-phase material originating from the dam body. The discharge at O2 (Thame Village) exhibits a delayed and attenuated yet still significant flood wave, arriving 880 s (~15 min) after the breach with maximum flow heights up to 4 m. This scenario highlights a comparatively slower-onset but high-volume failure process primarily driven by cumulative basin filling rather than instantaneous impact, resulting in a distinct hydrograph shape, lower travel time and potentially different downstream impacts compared with displacement-wave-triggered events.

The extent and depth of bed scour observed along the channel between the upper and lower lakes (Fig. 2) provide additional evidence that Scenario A is more plausible than Scenario B. Field observations reveal that a sand plain located immediately downstream of Thengpo Kharka, approximately 500 m long and 150 m wide, temporarily stored ponded water during the event (Fig. S8). Water released during GLOF event was briefly impounded within this sand plain, which likely attenuated the flood wave and delayed its downstream propagation. This phenomenon is accurately captured by the GLOF modelling, where water is shown to have been impounded just downstream of Thengpo Kharka (Figure 7). This temporary storage provided critical lead time for residents of Thame Village to evacuate safely. Subsequently, the impounded water overtopped and eroded the banks and bed of the ~2 km long channel between the ancient landslide dam and the debris fan near Thame Village, contributing to significant channel incision and sediment transport (Fig. S9).

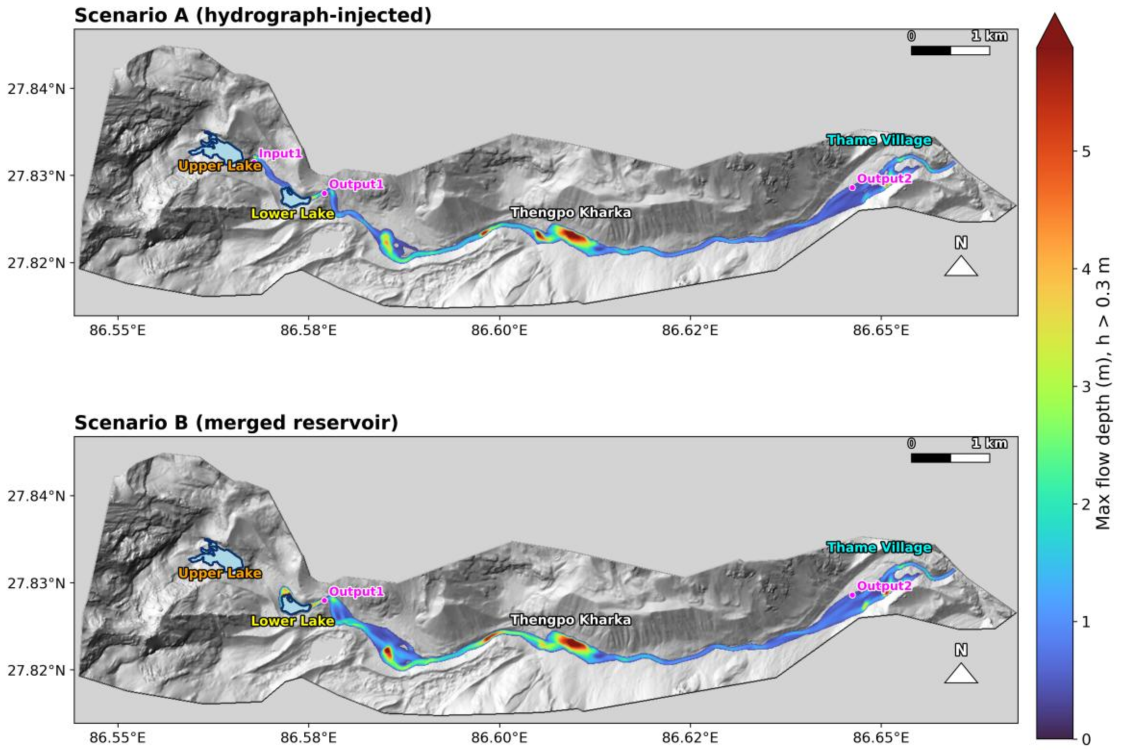

Figure 7: Simulation results of flow height (m) inundation for Scenario A and Scenario B. The background images are hill shade of HMA-DEM. Note: Only flow heights ≥ 30 cm are considered for visualization.

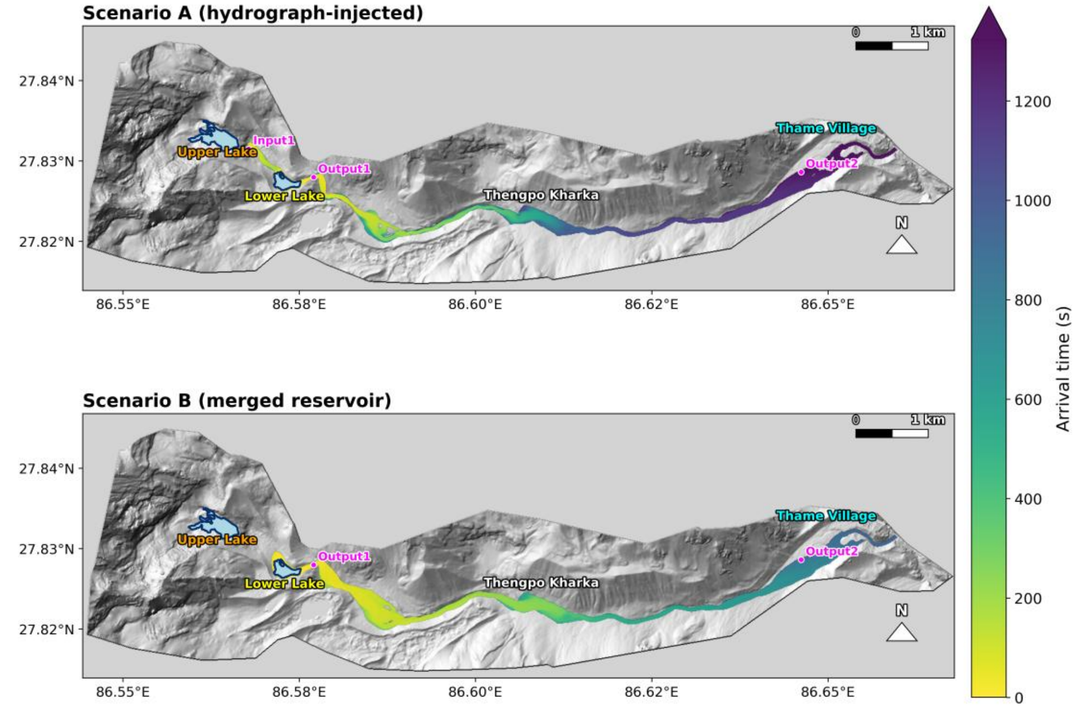

Figure 8: Simulation results of arrival times for Scenario A and Scenario B. The background images are hill shade of HMA-DEM.

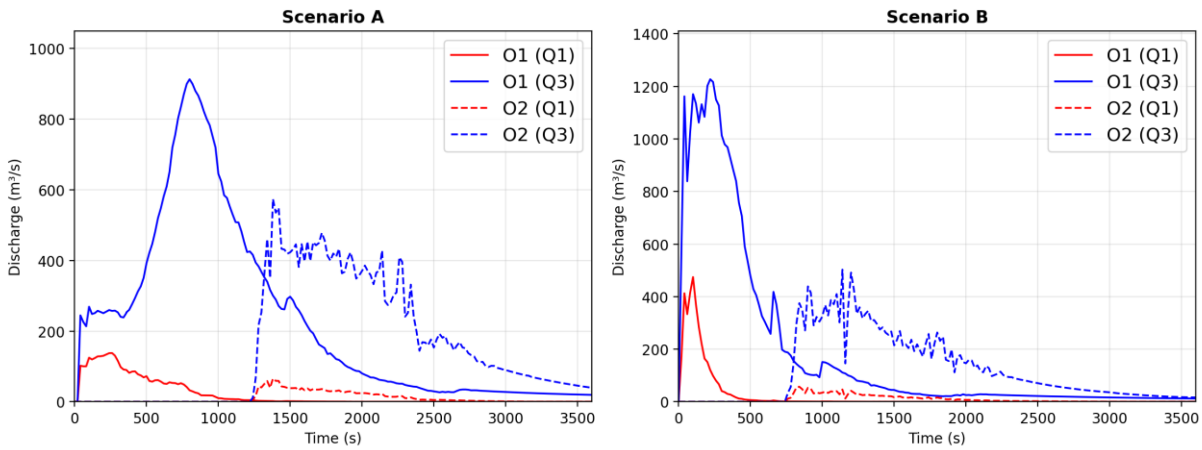

Figure 9: Hydrographs for Scenario A and Scenario B. Here, Q1 is solid phase and Q3 is fluid phase.

4.5 Downstream impacts of GLOF

The GLOF had profound impacts in the downstream areas as it turned into perilous debris flood with Thame Village being the primary deposition zone (Figure 10 and S9). The roaring sound of the flood and information flow from upstream to downstream areas helped the communities to evacuate during the GLOF event, leaving no casualties. The GLOF had a devastating impact on Thame Village, displacing 135 people and leading to the destruction of several tea houses and buildings, including the primary school, as well as considerable damage to agricultural fields (Figure 10). The detailed impact assessment shows that GLOF impacted the settlements, trekking trials, land and infrastructures worth total of 6.18 million USD in KPL RM alone (Table 6). The total length of trekking trail damaged in Thame Village was ~500 m cross-verified through images. The impacts of the GLOF were minimal outside the KPL RM; however, it caused substantial erosion and bank cutting up to 50 kilometres downstream and partially damaged a motorable bridge (Figure 10f).

The GLOF-triggered landslides in the Thame area, characterized by active glacio-lacustrine deposits, are ongoing. Deep-seated movement in Thame Village is exacerbated by riverbank erosion and migration (Fig. S10), leading to persistent ground settlement and tension cracking, particularly during wet periods. Elevated water levels during the monsoon further destabilize the slopes, with landslide activity expected to extend into areas farther from the river. Deep-seated rotational landslides are advancing from the east and north sides of the head pond on the right bank, impacting houses and agricultural land on the left bank.

Table 6. Impacts of GLOF on Khumbu Pashunglamu Rural Municipality.

Items	Loss description	Monetary amount*	Remarks
People	1 injured	-	No casualties; 135 displaced
Buildings Private house + Lodge + 1 primary school	45 owners	NRs. 560,874,214 USD 4,185,316	Loss including buildings, furniture and property inside
	1 School	NRs. 60,050,000 USD 448,101	Including school properties without land evaluation
Trekking Trails	1.2 km in different places	NRs. 3,019,382 USD 22,531	Maintenance costs
Private land	98920 m^2	204,847,183 USD 1,528,596	This includes agricultural and land property where there were buildings.
Micro-hydropower	Partial damage	-	The intake to desander and the pipes connecting them were damaged and was soon reconstructed and now is in operation
Bridges#	1	-	Motorable bridge was damaged 47 km downstream of Thame
Total		NRs. 82,879,780 USD 6,184,544	

#Outside KPL RM; *Exchange rate of 1 USD = NRs 134.01 based on Nepal Central Bank's 2024-08-18 rate (https://www.nrb.org.np/forex/)

Figure 10: Impacts of Thame Valley GLOF. Thame Valley (a) before and (b) after GLOF, (c) the damaged Thame school, walking trails (d and e) and the motorable bridge (f). The red arrows show common feature/buildings on panels (a) and (b).

Source: The picture (a) is sourced from © Google Earth 2024; images: © CNES/Airbus, Maxar Technologies, Airbus whereas others from Field Study, 2024.

5 Discussion

5.1 Evolution of glacial lake in response to climate change induced glacier retreat

Increase in temperatures in the Himalayan region are driving the retreat and mass loss of glacier (Bhattacharya et al., 2021) and subsequently new lakes are being emerged at higher elevation (>4,600 m a.s.l) in the Himalaya, including Nepal (Khadka et al., 2018). It is clearly visible in the satellite image that there is no existence of the upper lake before 2000 (Figure 3a). In the eastern Nepal including Everest region, maximum annual temperature has increased by 0.06°C per year (Salerno et al., 2015) and particularly, in the study area, the annual average temperature has increased by 0.17 °C per decade during 1994−2024 (Fig. 6d). In response to climatic warming, glaciers have retreated with rates of −6.1 ± 0.2 m yr^{-1} between 1962 and 2011 (Thakuri et al., 2014). The parent glacier of the upper lake has shrunk by −0.45 km^2 between 1980 and 2024 (Figure 3a), consequently the lake started to develop as glacier mass loss accelerated. After the development of the glacial lake, notable expansion occurred leading up to the outburst (Fig. S4).

5.2 Potential triggering factors of the upper lake outburst

Although mass movements (e.g., snow/ice avalanches, rockfalls, or landslides) trigger over 70 % of Himalayan GLOFs (Nie et al., 2018; Lützow et al., 2023), a probable snow/ice avalanche trigger was neither reported by government institutions or the Sagarmatha Pollution Control Committee during their immediate post-event field survey (Maharjan et al., 2025), nor was it evident in available remote sensing imagery. Through discounting other potential triggers (Table 5), our analysis indicates that the GLOF from upper lake was likely triggered by a rapid increase in the volume of the upper lake or a displacement wave, driven by extreme temperature-induced snow and glacier melt. The GLOF initiation potentially included calving from the parent glacier, although it is possible this calving occurred post-GLOF caused by the lake level lowering. Our analysis cannot definitively attribute the GLOF to a rockfall, as reported by ICIMOD (Maharjan et al., 2025).

High-resolution remote sensing images (Figure 5) and geomorphological/geological interpretation provides no definitive evidence of a contemporary rockfall or rockslides (Figure 11a) impacting the lake. The rock deposits observed along the eastern moraine margins are characterized by a dark, weathered appearance, inconsistent with the fresh, sandy or whitish talus typically associated with recent rock avalanches (Figure 11). Historical imagery and local accounts confirm these deposits were likely pre-existing (Fig. S5). All historical images (Fig. S5) depict a cluster of boulders that has been present since 2014. It appears that this section of the rockfall is partially situated on debris-covered ice that is melting, rather than directly on the lake bed. Furthermore, fresh small patches of scars observed in the north-eastern zone are an unlikely source for the GLOF (Figure 11b). The corresponding rockfall volume appears too small to generate a displacement wave capable of significantly impacting the main lake. Even if a wave were generated, the narrow strait would dampen its energy before it could propagate into the main lake. Additionally, the extreme verticality of the terrain limits the reliability of DEM differencing for detecting recent slope failures. Even if a rockfall had occurred as described by Maharjan et al. (2025), its direct impact on the lake is considered unlikely as a substantial already present debris apron (~20–30 m wide) buffers the lake from the lateral moraine slopes, intercepting material and preventing a direct, dynamic hit on the water body.

Therefore, we conclude that the GLOF from upper lake was most likely caused by a hydrological tipping point, a phenomenon that similarly contributed to the 2013 Kedarnath outburst-related disaster (Allen et al., 2016) and the 2009 outburst of Ventisquero Negro in the Patagonian Andes (Worni et al., 2012). Consecutive days of extreme precipitation and anomalously high temperatures prior to the event (Fig. 6) may have contributed to hydro-meteorological preconditioning prior of the lake system. Although direct observations of lake-level changes are unavailable and a causal relationship cannot be conclusively established (Fig. S11), the observed meteorological anomalies support the hypothesis that these conditions increased the lake's susceptibility to failure.

However, we acknowledge the possibility that a sudden rockfall or rock avalanche might have been occurred, as reported by Maharjan et al. (2025) who visited the site earlier than our team. Given the rapidly changing post-event conditions and the presence of steep, highly fragmented rock slopes along the eastern margin of the upper lake (Fig. 11), a rockfall or rock-avalanche remains plausible. Nevertheless, the available evidence is insufficient to constrain its timing or volume, or to determine whether the observed scour path represents a rockfall trajectory or erosion caused by flowing water into the lake. Notably, the cascading GLOF modelling, through its two scenarios effectively captures the range of possible outburst mechanisms and process (Sections 3.4 and 4.4), even when the exact triggering factor of the upper lake remains undefined.

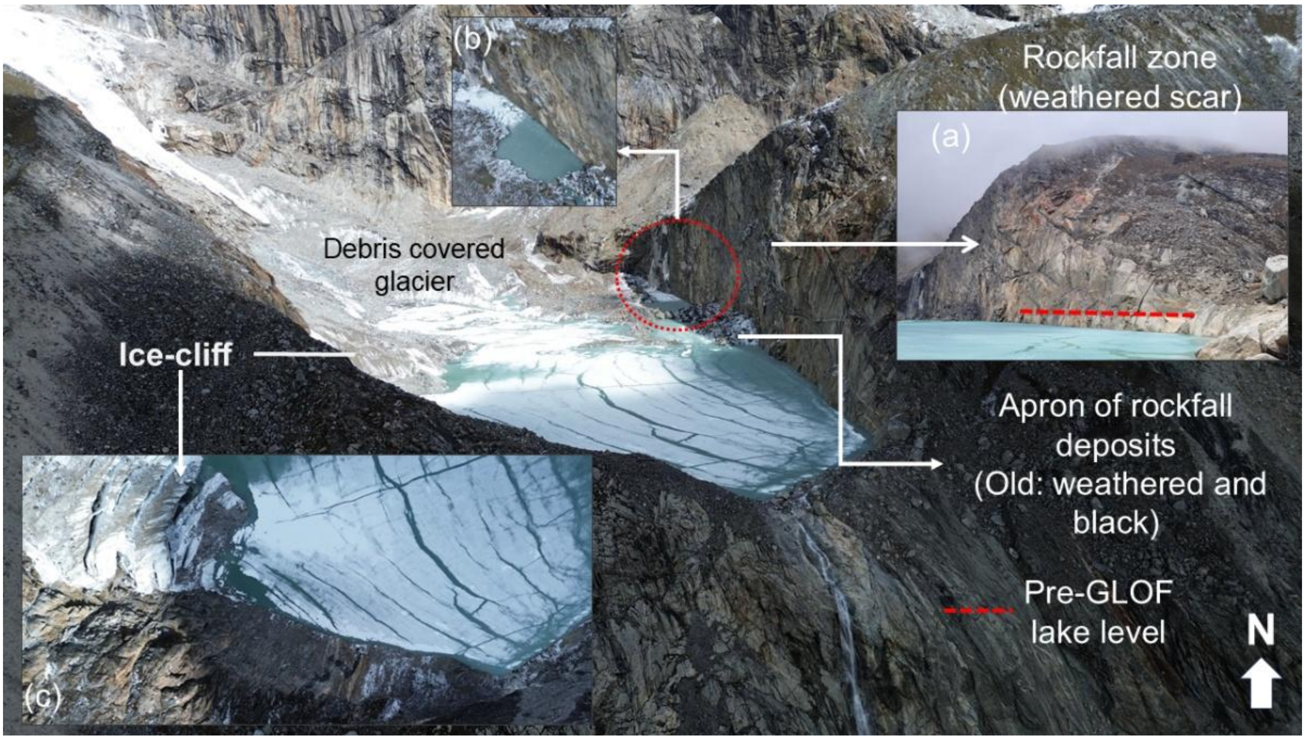

Figure 11: Bird eye view of upper lake with surrounding geology captured on May 2025. Photos: C. S. Watson, 2025

5.3 Implication and limitations of the modelling and study

The modelling demonstrates that small, previously overlooked glacial lakes can generate hazardous cascading outburst consequences when hydraulically connected. The simulations indicate that downstream impacts were controlled not only by the initial outburst volume but also by progressive lake interactions and sediment entrainment. These findings highlight the importance of considering multi-lake systems in future GLOF hazard assessments.

Comparison of the empirical and drone DEM-derived drained volume estimates (Text S1) shows good agreement for the lower lake, differing by only 2.9 %. In contrast, the empirical approach underestimated the upper lake drained volume by 64 %, resulting in a 28.3 % underestimation of the total drained volume (Text S1). This highlights the advantage of post-GLOF DEM-based reconstruction for estimating drained volume, particularly where lake basin morphology is complex. However, post-GLOF DEM-based drained volume reconstruction is also sensitive to lake outlines. The absence of high-resolution DEMs for the post-GLOF period precluded the incorporation of spatially heterogeneous parameter values and constrained the calibration of model inputs (Zhang et al., 2025). Consequently, the discharge and the simulated results by the model might be underestimated, particularly in the Thame Valley as compared to field—limitations attributable to the lack of fine resolution DEM, post-event topographic data and uncertainties associated with erosion (including large boulders) and deposition rates along the river channel (Fig. S9). This limitation is consistent with previously documented challenges in r.avaflow applications or any hydrodynamic models (Rinzin et al., 2025; Sattar et al., 2025b). Moreover, r.avaflow is sensitive to input parameters and adjusting them can affect mass flow behaviour (Mergili et al., 2018a). Future modelling studies can enhance debris flow dynamics by incorporating high-resolution DEMs along with erosion and deposition rates along the river channel. While alternative hydrodynamic models such as HEC-RAS may offer advantages in accurately reproducing inundation extents (Sattar et al., 2025b), metrics such as travel time and peak discharge are of greater relevance in the context of complex mass flows and cascading processes (Mergili et al., 2020a). In this regard, the performance of r.avaflow remains satisfactory and also the inundation extent produced by it when compared to post-GLOF images with acceptable F1 scores (Figure 7 *vs* Fig. S9). From a model-development perspective, this event highlights both the capability of r.avaflow to simulate complex cascading GLOF processes and the challenges associated with estimating drained lake volumes, and sediment availability and mobilisation. These findings emphasize the need for improved parameter constraints and high spatial resolution DEM for future applications. The GLOF modelling is limited to Thame Village; therefore, future studies could assess GLOF impacts further downstream.

On the impacts side, tangible loss is quantified in this study, however intangible impacts and losses such as cultural loss, mental and physical stress of GLOF is not covered by this study and needs a different evaluation and assessment approach.

5.4 Future GLOF hazard of upper and lower glacial lake

GLOF hazard refers to the likelihood and magnitude of an outburst event from a given lake, considering a broad range of contributing factors (Allen et al., 2022). In this context, both national (Rounce et al., 2017) and basin scale (Khadka et al., 2021) hazard assessments have overlooked the upper and lower lakes, primarily due to minimum size thresholds used in their studies (Table 1). The Thame event suggests that existing GLOF hazard assessment schemes should be revised in two key ways: (1) lake-size thresholds used to screen potentially dangerous lakes should be lowered to include small lakes capable of producing damaging outbursts, and (2) assessments should explicitly evaluate cascading processes, whereby failure of an upstream lake can trigger downstream lake outbursts and amplify flood impacts. To address this gap, a first-order assessment of future GLOF hazard for both lakes was systematically conducted by analysing twenty GLOF hazard factors (GAPHAZ, 2017) that encompass atmospheric, cryospheric, geotechnical and geomorphological, conditioning and triggering variables (Table S4).

A repeated GLOF from the upper lake is possible, since it is still connected to a calving glacier, has potential for upward expansion and remains susceptible to ice/snow avalanches and rockfall (Figure 11). Following the 2024 event, however, much of the moraine and debris that previously formed the dam was removed, leaving the lake largely confined by bedrock.

As a result, the likelihood of a dam breach failure similar to that of 2024 event is reduced. Nevertheless, overtopping induced by displacement waves generated by ice or rock avalanches cannot be ruled out, particularly as a substantial proportion of the upper lake volume remains. In contrast, the lower lake has lost ~ 80% of its volume in the recent event (Table S1). It no longer has direct contact with a glacier (Figure 1) and is not susceptible to direct ice- or rock-fall triggers. Although a renewed outburst remains possible if a GLOF were to originate from the upper lake, the reduced lower lake volume suggests that the magnitude of future cascading floods is likely to be lower than that of the 2024 event in the near term. Continued glacier retreat and future lake evolution may, however, alter the hazard potential over longer timescales. Therefore, regular monitoring of upper glacial lake is recommended using remote sensing technologies and field assessments.

5.5 Disaster risk management in Thame Valley

The Thame GLOF event underscores the need for proactive, integrated disaster risk management that addresses compound hazards in the Thame Valley, including glacio-lacustrine landslides, monsoon-driven flooding, channel instability, and potential future GLOFs from small lakes (Sattar et al., 2025a). Risk in the valley arises not only from the probability of extreme outburst floods but also from the interaction of ongoing geomorphic processes with settlements and critical infrastructure along the Thame stream (Fig. S10). Effective risk management must therefore integrate hazard assessment, exposure reduction, and vulnerability mitigation within a unified framework (Emmer, 2024; Niggli et al., 2024; Wang et al., 2026).

Short-term measures should focus on reducing hazard impacts and immediate exposure rather than attempting to eliminate underlying geomorphic drivers. Targeted structural interventions—such as selective, over-toppable flow-diversion berms near the debris-fan apex and localized bank protection within the village—can help limit flood intrusion and channel migration under recurrent monsoon conditions. Concurrently, GLOF exposure and vulnerability must be reduced through land-use restrictions or zoning, evacuation of structurally compromised buildings and systematic ground deformation monitoring. Low-cost monitoring approaches can support adaptive decision-making, including evacuation thresholds and infrastructure relocation, while large-scale river engineering works are not recommended due to high cost, technical uncertainty, and limited long-term effectiveness.

Over the long term, sustainable GLOF risk reduction depends primarily on exposure management through risk-informed land-use planning and the progressive relocation of permanent settlements and critical infrastructure to lower-hazard zones (Khadka et al., 2024a). Areas subject to frequent flooding or landsliding should be reserved for low-exposure areas. Given persistent residual risk, a robust GLOF early warning system is also essential to reduce vulnerability and prevent loss of life. Such a system must combine reliable hydrological monitoring, communication mechanisms with redundancy, clear evacuation planning, and strong institutional support for maintenance and periodic reassessment (Wang et al., 2026). Overall, the Thame case highlights that in high-mountain environments, reducing GLOF exposure and vulnerability is more effective than attempting to fully control dynamic geomorphic hazards and implementing expensive lake mitigation projects such as lake lowering.

6 Conclusions

This study provides a comprehensive analysis of the cascading GLOF event in the Thame Valley on August 16, 2024, an event originating from relatively small, often overlooked, glacial lakes in the headwaters. By integrating multi-source remote sensing, climatic data, numerical modelling, field assessments, and government reports, we reconstructed and evaluated the process chain of this event, potential mechanisms, and downstream impacts.

Our findings reveal that the GLOF was a direct consequence of rapid and ongoing cryospheric change. The upper glacial lake experienced significant expansion in recent years due to climate-induced glacier retreat. The immediate trigger for its outburst was likely a combination of extremes of temperature and precipitation, surpassing the 90th and 95th percentiles of historical records, which drove rapid melt and ice-calving into the lake. This initial failure released a flood that, in turn, breached the lower glacial lake, creating a cascading GLOF process. A combined volume of approximately 7.7×10^5 m^3 of water was released. Post-event, the surface area of the upper lake decreased by 0.013 km^2, while the lower lake was reduced from 0.048 ± 0.01 km^2 to 0.015 km^2.

Numerical modelling using the r.avaflow mass flow model, which considered two likely scenarios, successfully reconstructed the event dynamics. The simulation indicates that the heterogenous flood wave reached a maximum of 8 m along the river channel. Comparison with field observations, particularly the extent and depth of channel scour between the upper and lower lakes, indicates that Scenario A, involving dam overtopping, is the more plausible reconstruction of the event. The definitive cause of this overtopping is not known; however, our analysis points to a hydrological tipping point driven by intense glacier melt and calving associated with extreme temperatures and precipitation. A rock avalanche from the steep, highly fragmented slopes surrounding the upper lake may have contributed to overtopping and initiation of the outburst. Nevertheless, additional investigations are needed to confirm the triggering mechanism. The flood wave reached Thame Valley within 22 minutes of the initial outburst, transitioning into a highly destructive debris flow as it propagated downstream. Although no casualties were reported, the socio-economic impact was substantial, causing an estimated 6.18 million USD in damage to settlements, trekking routes, and infrastructure in 2024.

The Thame Valley event reveals a critical gap in current GLOF risk assessment paradigms: the underestimated hazard of rapidly evolving small high-mountain lakes, particularly when they form cascading systems along a single channel. This disaster exemplifies the direct linkage between climate change, glacier retreat, and the generation of downstream hazards. Consequently, we argue for a strategic shift in risk management. In such dynamic high-mountain environments, priority should be given to reducing the exposure and vulnerability of downstream communities and infrastructure, rather than focusing solely on the technically challenging and often ineffective task of mitigating GLOFs at their source or attempting to control the geomorphic hazards themselves. Future GLOF risk assessments should therefore prioritize the systematic monitoring of all glacial lakes, regardless of size, as well as settlements located along river channels that may be vulnerable to cascading events.

Supplement. The supplement related to this article has been submitted for review.

Code and Data availability

The mass flow simulation tool, r.avaflow used for GLOF modelling is freely available at https://www.landslidemodels.org/r.avaflow/ (Mergili and Pudasaini, 2014-2025). Landsat data is sourced from https://earthexplorer.usgs.gov/, Sentinel-2 from https://browser.dataspace.copernicus.eu/ and HMA DEM from https://nsidc.org/data/ whereas ERA5-Land data are obtained from Google Earth Engine (https://earthengine.google.com). The ice thickness data was obtained from https://doi.org/10.3929/ethz-b-000315707. Additional commercial and closed access datasets used are available from the corresponding or lead authors on request.

Author contributions

NK and VPP developed the idea with inputs from GZ. NK, KS, CSW and LDR conducted field studies differently in October-December 2024 and May 2025. NK collected required data from GZ, CSW, KB, LDR and DS. NK developed the manuscript with inputs from TW and MRG in the GLOF simulations and under supervision of VPP. All authors contributed in the discussion, revision and editing of the manuscript and approved the final draft.

Competing interests

The authors declare that they have no conflict of interest.

Acknowledgement

The authors would like to acknowledge 'ReCAP - Developing MH risk assessment model and supporting the design of MHEWS approach in Nepal' project funded by SDC as well as 'Collaborative Research and Capacity Strengthening for Enhancing Water Security (CaREWaS)' project funded by Kathmandu Valley Water Supply Management Board for supporting NK, VPP and SA. Further, it builds on the field study to Thame on October-November 2024 supported by IMHE-CAS to NK. The contribution of GZ was supported by the National Natural Science Foundation of China (42301140, 42571150) and the National Key Research and Development Program of China (2024YFF0808603). KS gratefully acknowledges the support of the Asian Development Bank (ADB) and NDRRMA, Nepal in facilitating the field visit to Thame under the Building Adaptation and Resilience in the Hindu Kush Himalaya (BARHKH) project. NK thanks Archana Ghimire (KPL RM Environment officer) and K. Dahal for thier help. CSW is supported by a UKRI Future Leaders Fellowship [grant number MR/Y016564/1]. Figure 2a was converted to 3D using ChatGPT.

References

Allen, S. K., Rastner, P., Arora, M., Huggel, C., and Stoffel, M.: Lake outburst and debris flow disaster at Kedarnath, June 2013: hydrometeorological triggering and topographic predisposition, Landslides, 13, 1479-1491, https://doi.org/10.1007/s10346-015-0584-3, 2016.

Allen, S. K., Zhang, G., Wang, W., Yao, T., and Bolch, T.: Potentially dangerous glacial lakes across the Tibetan Plateau revealed using a large-scale automated assessment approach, Sci Bull, 64, 435-445, https://doi.org/10.1016/j.scib.2019.03.011, 2019.

Allen, S. K., Sattar, A., King, O., Zhang, G., Bhattacharya, A., Yao, T., and Bolch, T.: Glacial lake outburst flood hazard under current and future conditions: worst-case scenarios in a transboundary Himalayan basin, Natural Hazards and Earth System Sciences, 22, 3765-3785, https://doi.org/10.5194/nhess-22-3765-2022, 2022.

Bajracharya, S. R., Shrestha, A. B., Shrestha, F., Wagle, N., Maharjan, S. B., and Sherpa, T. C.: Inventory of glacial lakes and identification of potentially dangerous glacial lakes in the Koshi, Gandaki, and Karnali river basins of Nepal, the Tibet autonomous region of China, and India, International Centre for Integrated Mountain Development (ICIMOD); United Nations Development Programme (UNDP), Kathmandu, Nepal, 54, 10.53055/ICIMOD.773, 2020.

Bhattacharya, A., Bolch, T., Mukherjee, K., King, O., Menounos, B., Kapitsa, V., Neckel, N., Yang, W., and Yao, T.: High Mountain Asian glacier response to climate revealed by multi-temporal satellite observations since the 1960s, Nature communications, 12, 4133, https://doi.org/10.1038/s41467-021-24180-y, 2021.

Byers, A. C.: Khumbu since 1950: cultural, landscape, and climate change in the Sagarmatha (Mt. Everest) National Park, Khumbu, Nepal, Alton C. Byers2017.

Byers, A. C., Rounce, D. R., Shugar, D. H., Lala, J. M., Byers, E. A., and Regmi, D.: A rockfall-induced glacial lake outburst flood, Upper Barun Valley, Nepal, Landslides, 1-17, https://doi.org/10.1007/s10346-018-1079-9, 2018.

Chen, H., Liang, Q., Zhao, J., and Maharjan, S. B.: Assessing national exposure to and impact of glacial lake outburst floods considering uncertainty under data sparsity, Hydrol. Earth Syst. Sci., 29, 733-752, 10.5194/hess-29-733-2025, 2025.

Chen, H., Wu, T., Li, S., Chen, J., Ruan, H., Li, X., and Mou, Y.: New insights on the 2020 Jinwuco glacial lake outburst flood: considering ice content within the moraine dam, Geomatics, Natural Hazards and Risk, 17, 2649567, 10.1080/19475705.2026.2649567, 2026.

Chen, N., Liu, M., Allen, S., Deng, M., Khanal, N. R., Peng, T., Tian, S., Huggel, C., Wu, K., Rahman, M., and Somos-Valenzuela, M.: Small outbursts into big disasters: Earthquakes exacerbate climate-driven cascade processes of the glacial lakes failure in the Himalayas, Geomorphology, 422, 108539, 10.1016/j.geomorph.2022.108539, 2023.

Chen, Y., Sharma, S., Zhou, X., Yang, K., Li, X., Niu, X., Hu, X., and Khadka, N.: Spatial performance of multiple reanalysis precipitation datasets on the southern slope of central Himalaya, Atmospheric Research, 250, 105365, 2021.

Cook, K. L., Andermann, C., Gimbert, F., Adhikari, B. R., and Hovius, N.: Glacial lake outburst floods as drivers of fluvial erosion in the Himalaya, Science, 362, 53-57, 2018.

Cook, S. and Quincey, D.: Estimating the volume of Alpine glacial lakes, Earth Surface Dynamics, 3, 559, 2015.

Costa, J. E.: Floods from dam failures, 560, US Geological Survey1985.

COSTA, J. E. and SCHUSTER, R. L.: The formation and failure of natural dams, GSA Bulletin, 100, 1054-1068, 10.1130/0016-7606(1988)100<1054:TFAFON>2.3.CO;2 %J GSA Bulletin, 1988.

Cuellar, A. D. and McKinney, D. C.: Decision-Making Methodology for Risk Management Applied to Imja Lake in Nepal, Water, 9, 591, 2017.

Dubey, S. and Goyal, M. K.: Glacial Lake Outburst Flood Hazard, Downstream Impact, and Risk Over the Indian Himalayas, Water Resources Research, 56, e2019WR026533, 2020.

Emmer, A.: Understanding the risk of glacial lake outburst floods in the twenty-first century, Nature Water, 2, 608-610, https://doi.org/10.1038/s44221-024-00254-1, 2024.

Evans, S. G.: The maximum discharge of outburst floods caused by the breaching of man-made and natural dams, Canadian Geotechnical Journal, 23, 385-387, 10.1139/t86-053, 1986.

Froehlich, D.: Predicting Peak Discharge of Outburst Floods from Moraine-Dammed Glacial Lakes, Natural Hazards Review, 26, 04025047, https://doi.org/10.1061/NHREFO.NHENG-2492, 2025.

Froehlich, D. C.: Peak outflow from breached embankment dam, Journal of water Resources Planning and management, 121, 90-97, 1995.

Furian, W. and Sauter, T.: Assessing economic impacts of future GLOFs in Nepal's Everest region under different SSP scenarios using three-dimensional simulations, Nat. Hazards Earth Syst. Sci., 25, 3779-3802, https://doi.org/10.5194/nhess-25-3779-2025, 2025.

Furian, W., Loibl, D., and Schneider, C.: Future glacial lakes in High Mountain Asia: an inventory and assessment of hazard potential from surrounding slopes, Journal of Glaciology, 67, 653-670, https://doi.org/10.1017/jog.2021.18, 2021.

GAPHAZ: Assessment of Glacier and Permafrost Hazards in Mountain Regions – Technical Guidance Document. , Zurich, Switzerland / Lima, Peru, , 72, 2017.

Ghimire, B.: Aerial inspection ties Thame flood to glacial lake outburst, The Kathmandu Post, https://kathmandupost.com/climate-environment/2024/08/18/aerial-inspection-ties-thame-flood-to-glacial-lake-outburst Last Accessed 05/04/2026, 2024.

Gouli, M. R., Hu, K., Khadka, N., Liu, S., Yifan, S., Adhikari, M., and Talchabhadel, R.: Quantitative assessment of the GLOF risk along China-Nepal transboundary basins by integrating remote sensing, machine learning, and hydrodynamic model, International Journal of Disaster Risk Reduction, 118, 105231, 10.1016/j.ijdrr.2025.105231, 2025.

Hu, J., Yao, X., Duan, H., Zhang, Y., Wang, Y., and Wu, T.: Temporal and Spatial Changes and GLOF Susceptibility Assessment of Glacial Lakes in Nepal from 2000 to 2020, Remote Sensing, 14, 5034, 2022.

Huggel, C., Kääb, A., Haeberli, W., Teysseire, P., and Paul, F.: Remote sensing based assessment of hazards from glacier lake outbursts: a case study in the Swiss Alps, Canadian Geotechnical Journal, 39, 316-330, http://www.nrcresearchpress.com/doi/pdfplus/10.1139/t01-099, 2002.

ICIMOD: Glacial Lakes and Glacial Lake Outbursts Floods in Nepal ICIMOD, Kathmandu, 99, 2011.

Kapitsa, V., Shahgedanova, M., Machguth, H., Severskiy, I., and Medeu, A.: Assessment of evolution and risks of glacier lake outbursts in the Djungarskiy Alatau, Central Asia, using Landsat imagery and glacier bed topography modelling, Nat. Hazards Earth Syst. Sci., 17, 1837-1856, https://doi.org/10.5194/nhess-17-1837-2017, 2017.

Khadka, N., Zhang, G., and Chen, W.: The state of six dangerous gla-cial lakes in the Nepalese Himalaya, Terr. Atmos. Ocean. Sci, 30, 63-72, 2019.

Khadka, N., Zhang, G., and Thakuri, S.: Glacial lakes in the Nepal Himalaya: Inventory and decadal dynamics (1977–2017), Remote Sensing, 10, 1913, https://doi.org/10.3390/rs10121913, 2018.

Khadka, N., Chen, X., Sharma, S., and Shrestha, B.: Climate change and its impacts on glaciers and glacial lakes in Nepal Himalayas, Regional Environmental Change, 23, 143, https://doi.org/10.1007/s10113-023-02142-y, 2023.

Khadka, N., Chen, X., Shrestha, M., and Liu, W.: Risk perception and vulnerability of communities in Nepal to transboundary glacial lake outburst floods from Tibet, China, International Journal of Disaster Risk Reduction, 107, 104476, https://doi.org/10.1016/j.ijdrr.2024.104476, 2024a.

Khadka, N., Chen, X., Yong, N., Thakuri, S., Zheng, G., and Zhang, G.: Evaluation of Glacial Lake Outburst Flood susceptibility using multi-criteria assessment framework in Mahalangur Himalaya, Frontiers in Earth Science, 8, 748, https://doi.org/10.3389/feart.2020.601288, 2021.

Khadka, N., Zheng, G., Chen, X., Zhong, Y., Allen, S. K., and Gouli, M. R.: An ice-snow avalanche triggered small glacial lake outburst flood in Birendra Lake, Nepal Himalaya, Natural Hazards, 121, 6357-6365, https://doi.org/10.1007/s11069-024-07014-0, 2024b.

Khanal, N. R., Mool, P. K., Shrestha, A. B., Rasul, G., Ghimire, P. K., Shrestha, R. B., and Joshi, S. P.: A comprehensive approach and methods for glacial lake outburst flood risk assessment, with examples from Nepal and the transboundary area, International Journal of Water Resources Development, 31, 219-237, https://doi.org/10.1080/07900627.2014.994116, 2015.

King, O., Quincey, D. J., Carrivick, J. L., and Rowan, A. V.: Spatial variability in mass loss of glaciers in the Everest region, central Himalayas, between 2000 and 2015, The Cryosphere, 11, 407-426, 2017.

Lala, J. M., Rounce, D. R., and McKinney, D. C.: Modeling the glacial lake outburst flood process chain in the Nepal Himalaya: reassessing Imja Tsho's hazard, Hydrology and Earth System Sciences, 22, 3721-3737, 2018.

Lamsal, D., Sawagaki, T., Watanabe, T., Byers, A. C., and McKinney, D. C.: An assessment of conditions before and after the 1998 Tam Pokhari outburst in the Nepal Himalaya and an evaluation of the future outburst hazard, Hydrological Processes, 30, 676-691, 2016.

Lee, E., Carrivick, J. L., Quincey, D. J., Cook, S. J., James, W. H., and Brown, L. E.: Accelerated mass loss of Himalayan glaciers since the Little Ice Age, Scientific reports, 11, 24284, https://doi.org/10.1038/s41598-021-03805-8, 2021.

Lützow, N., Veh, G., and Korup, O.: A global database of historic glacier lake outburst floods, Earth System Science Data, 15, 2983-3000, 10.5194/essd-15-2983-2023, 2023.

Maharjan, S. B., Sherpa, T. C., and Shrestha, A. B.: Thame Valley Glacial Lake Outburst Flood 2024: Causes, impacts and future risks, ICIMOD, NDRRMA https://doi.org/10.53055/ICIMOD.1101, Kathmandu, 2025.

Majeed, U., Rashid, I., Sattar, A., Allen, S., Stoffel, M., Nüsser, M., and Schmidt, S.: Recession of Gya Glacier and the 2014 glacial lake outburst flood in the Trans-Himalayan region of Ladakh, India, Science of The Total Environment, 756, 144008, 2021.

r. avaflow–The mass flow simulation tool https://www.avaflow.org, last

Mergili, M., Fischer, J.-T., Krenn, J., and Pudasaini, S. P.: r. avaflow v1, an advanced open-source computational framework for the propagation and interaction of two-phase mass flows, Geoscientific Model Development, 10, 553-569, https://doi.org/10.5194/gmd-10-553-2017, 2017.

Mergili, M., Jaboyedoff, M., Pullarello, J., and Pudasaini, S. P.: Back calculation of the 2017 Piz Cengalo–Bondo landslide cascade with r.avaflow: what we can do and what we can learn, Nat. Hazards Earth Syst. Sci., 20, 505-520, 10.5194/nhess-20-505-2020, 2020a.

Mergili, M., Pfeffer, H., Kellerer-Pirklbauer, A., Zangerl, C., and Pudasaini, S. P.: r. avaflow v4, a multi-purpose landslide simulation framework, Geoscientific Model Development, 18, 9879-9896, https://doi.org/10.5194/gmd-18-9879-2025, 2025.

Mergili, M., Pudasaini, S. P., Emmer, A., Fischer, J.-T., Cochachin, A., and Frey, H.: Reconstruction of the 1941 GLOF process chain at lake Palcacocha (Cordillera Blanca, Peru), Hydrology and Earth System Sciences, 24, 93-114, 2020b.

Mergili, M., Emmer, A., Juřicová, A., Cochachin, A., Fischer, J.-T., Huggel, C., and Pudasaini, S. P.: How well can we simulate complex hydro-geomorphic process chains? The 2012 multi-lake outburst flood in the Santa Cruz Valley (Cordillera Blanca, Perú), 43, 1373-1389, https://doi.org/10.1002/esp.4318, 2018a.

Mergili, M., Emmer, A., Juřicová, A., Cochachin, A., Fischer, J. T., Huggel, C., and Pudasaini, S. P.: How well can we simulate complex hydro-geomorphic process chains? The 2012 multi-lake outburst flood in the Santa Cruz Valley (Cordillera Blanca, Perú), Earth surface processes and landforms, 43, 1373-1389, https://doi.org/10.1002/esp.4318, 2018b.

Munch, J., Steiner, J., Huggel, C., Basniat, A., Pandey, V. P., Adhikari, B. R., Aaron, J., Mergili, M., and Allen, S. K.: Modeling Cascading Hazards in High Mountain Environments: Challenges and Approaches from the Thame Case Study, Nepal, EGU General Assembly 2026, Austria https://doi.org/10.5194/egusphere-egu26-17163,

Muñoz-Sabater, J., Dutra, E., Agustí-Panareda, A., Albergel, C., Arduini, G., Balsamo, G., Boussetta, S., Choulga, M., Harrigan, S., and Hersbach, H. J. E. s. s. d.: ERA5-Land: A state-of-the-art global reanalysis dataset for land applications, 13, 4349-4383, 2021.
National Statistic Office, N.: National Population and Housing Census 2021 (National Report) National Statistic Office, Government of Nepal Kathmandu (https://censusnepal.cbs.gov.np/results/files/result-folder/National%20Report_English.pdf), 2023.
Nie, Y., Liu, W., Liu, Q., Hu, X., and Westoby, M. J.: Reconstructing the Chongbaxia Tsho glacial lake outburst flood in the Eastern Himalaya: Evolution, process and impacts, Geomorphology, 370, 107393, 2020.
Nie, Y., Liu, Q., Wang, J., Zhang, Y., Sheng, Y., and Liu, S.: An inventory of historical glacial lake outburst floods in the Himalayas based on remote sensing observations and geomorphological analysis, Geomorphology, 308, 91-106, 2018.
Niggli, L., Allen, S., Frey, H., Huggel, C., Petrakov, D., Raimbekova, Z., Reynolds, J., and Wang, W.: GLOF Risk Management Experiences and Options: A Global Overview, Oxford Research Encyclopedia of Natural Hazard Science, https://doi.org/10.1093/acrefore/9780199389407.013.540, 2024.
Popov, N.: Assessment of glacial debris flow hazard in the north Tien-Shan, Proceedings of the Soviet-China-Japan Symposium and field workshop on natural disasters, 384-391,
Poudel, U., Gouli, M. R., Hu, K., Khadka, N., Regmi, R. K., and Thapa, B. R.: Multi-breach GLOF hazard and exposure analysis of Birendra Lake in the Manaslu Region of Nepal, Natural Hazards Research, 5, 800-813, 10.1016/j.nhres.2025.03.007, 2025.
Pudasaini, S. P. and Mergili, M.: A multi-phase mass flow model, Journal of Geophysical Research: Earth Surface, 124, 2920-2942, https://doi.org/10.1029/2019JF005204, 2019.
Rawlins, L. D., Watson, C. S., Bhambri, R., Khadka, N., and Chand, M. B.: Glacial Lake Observatory (GLO): annual dataset of glacial lakes in Nepal and transboundary catchments (2017–2024), Earth Syst. Sci. Data, 18, 5143-5165, 10.5194/essd-18-5143-2026, 2026.
Rinzin, S., Dunning, S., Carr, R. J., Sattar, A., and Mergili, M.: Exploring implications of input parameter uncertainties in glacial lake outburst flood (GLOF) modelling results using the modelling code r.avaflow, Nat. Hazards Earth Syst. Sci., 25, 1841-1864, 10.5194/nhess-25-1841-2025, 2025.
Rinzin, S., Zhang, G., Sattar, A., Wangchuk, S., Allen, S. K., Dunning, S., and Peng, M.: GLOF hazard, exposure, vulnerability, and risk assessment of potentially dangerous glacial lakes in the Bhutan Himalaya, Journal of Hydrology, 619, 129311, https://doi.org/10.1016/j.jhydrol.2023.129311, 2023.
Rounce, D. R., Watson, C. S., and McKinney, D. C.: Identification of hazard and risk for glacial lakes in the Nepal Himalaya using satellite imagery from 2000–2015, Remote Sensing, 9, 654, https://doi.org/10.3390/rs9070654, 2017.
Sakai, A.: Glacial lakes in the Himalayas: a review on formation and expansion processes, Global Environmental Research, 16, 23-30, 2012.
Salerno, F., Thakuri, S., D'Agata, C., Smiraglia, C., Manfredi, E. C., Viviano, G., and Tartari, G.: Glacial lake distribution in the Mount Everest region: Uncertainty of measurement and conditions of formation, Global and Planetary Change, 92, 30-39, 2012.
Salerno, F., Guyennon, N., Thakuri, S., Viviano, G., Romano, E., Vuillermoz, E., Cristofanelli, P., Stocchi, P., Agrillo, G., and Ma, Y.: Weak precipitation, warm winters and springs impact glaciers of south slopes of Mt. Everest (central Himalaya) in the last 2 decades (1994–2013), The Cryosphere, 9, 1229-1247, 2015.
Sattar, A., Haritashya, U. K., Kargel, J. S., and Karki, A.: Transition of a small Himalayan glacier lake outburst flood to a giant transborder flood and debris flow, Sci Rep, 12, 12421, 10.1038/s41598-022-16337-6, 2022.
Sattar, A., Emmer, A., Lhazom, T., Rai, S. K., and Azam, M. F.: Flood risk from small mountain lakes, Communications Earth & Environment, 6, 785, 10.1038/s43247-025-02758-4, 2025a.
Sattar, A., Goswami, A., Kulkarni, A. V., Emmer, A., Haritashya, U. K., Allen, S., Frey, H., and Huggel, C.: Future glacial lake outburst flood (GLOF) hazard of the South Lhonak Lake, Sikkim Himalaya, Geomorphology, 388, 107783, https://doi.org/10.1016/j.geomorph.2021.107783, 2021.
Sattar, A., Cook, K. L., Rai, S. K., Berthier, E., Allen, S., Rinzin, S., de Vries, M. V. W., Haeberli, W., Kushwaha, P., Shugar, D. H., Emmer, A., Haritashya, U. K., Frey, H., Rao, P., Gurudin, K. S. K., Rai, P., Rajak, R., Hossain, F., Huggel, C., Mergili, M., Azam, M. F., Gascoin, S., Carrivick, J. L., Bell, L. E., Ranjan, R. K., Rashid, I., Kulkarni, A. V., Petley, D., Schwanghart, W., Watson, C. S., Islam, N., Gupta, M. D., Lane, S. N., and Bhat, S. Y.: The Sikkim flood of October 2023: Drivers, causes, and impacts of a multihazard cascade, Science, 387, eads2659, 10.1126/science.ads2659, 2025b.
Sharma, S., Hamal, K., Khadka, N., and Joshi, B. B.: Dominant pattern of year-to-year variability of summer precipitation in Nepal during 1987–2015, Theoretical and Applied Climatology, 142, 1071-1084, 10.1007/s00704-020-03359-1, 2020.
Singh, A., Shrestha, D., Ghimire, K., Mishra, S., Rana, D., and Acharya, S.: Assessing machine learning models to generate permafrost distribution map in Solukhumbu, Nepal, Geodesy and Geodynamics, 16, 275-287, https://doi.org/10.1016/j.geog.2024.08.003, 2025.
Tai, Y.-C., Noelle, S., Gray, J., and Hutter, K. J. J. o. C. P.: Shock-capturing and front-tracking methods for granular avalanches, Journal of Computational Physics, 175, 269-301, https://doi.org/10.1006/jcph.2001.6946, 2002.

Thakuri, S., Salerno, F., Smiraglia, C., Bolch, T., D'Agata, C., Viviano, G., and Tartari, G.: Tracing glacier changes since the 1960s on the south slope of Mt. Everest (central Southern Himalaya) using optical satellite imagery, The Cryosphere, 8, 1297-1315, 2014.

Veh, G., Korup, O., and Walz, A.: Hazard from Himalayan glacier lake outburst floods, Proc Natl Acad Sci U S A, 117, 907-912, 10.1073/pnas.1914898117, 2020.

Veh, G., Wang, B. G., Zirzow, A., Schmidt, C., Lützow, N., Steppat, F., Zhang, G., Vogel, K., Geertsema, M., Clague, J. J., and Korup, O.: Progressively smaller glacier lake outburst floods despite worldwide growth in lake area, Nature Water, 3, 271-283, https://doi.org/10.1038/s44221-025-00388-w, 2025.

Vuichard, D. and Zimmermann, M.: The 1985 catastrophic drainage of a moraine-dammed lake, Khumbu Himal, Nepal: cause and consequences, Mountain Research and Development, 91-110, 1987.

Wang, X., Liu, S., Ding, Y., Guo, W., Jiang, Z., Lin, J., and Han, Y.: An approach for estimating the breach probabilities of moraine-dammed lakes in the Chinese Himalayas using remote-sensing data, Natural Hazards and Earth System Sciences, 12, 3109-3122, 2012.

Wang, X., Zhang, G., Veh, G., Sattar, A., Wang, W., Allen, S. K., Bolch, T., Peng, M., and Xu, F.: Reconstructing glacial lake outburst floods in the Poiqu River basin, central Himalaya, Geomorphology, 109063, https://doi.org/10.1016/j.geomorph.2024.109063, 2024.

Wang, X., Guo, X., Yang, C., Liu, Q., Wei, J., Zhang, Y., Liu, S., Zhang, Y., Jiang, Z., and Tang, Z.: Glacial lake inventory of high-mountain Asia in 1990 and 2018 derived from Landsat images, Earth System Science Data, 12, 2169-2182, https://doi.org/10.5194/essd-12-2169-2020, 2020.

Wang, X., Chen, W., Zhang, G., Emmer, A., Frey, H., Taylor, C., Huggel, C., Sattar, A., Zheng, G., Rashid, I., Carrivick, J. L., Veh, G., Allen, S., Steiner, J., Quincey, D., and Mergili, M.: Mitigating future glacial lake outburst floods in the Himalaya, Science Bulletin, 71, 159-171, https://doi.org/10.1016/j.scib.2025.11.024, 2026.

Watson, C. S., Kargel, J. S., Shugar, D. H., Haritashya, U. K., Schiassi, E., and Furfaro, R.: Mass loss from calving in Himalayan proglacial lakes, Frontiers in Earth Science, 7, 2020.

Westoby, M. J., Glasser, N. F., Hambrey, M. J., Brasington, J., Reynolds, J. M., and Hassan, M. A. A. M.: Reconstructing historic Glacial Lake Outburst Floods through numerical modelling and geomorphological assessment: Extreme events in the Himalaya, 39, 1675-1692, https://doi.org/10.1002/esp.3617, 2014.

Worni, R., Stoffel, M., Huggel, C., Volz, C., Casteller, A., and Luckman, B.: Analysis and dynamic modeling of a moraine failure and glacier lake outburst flood at Ventisquero Negro, Patagonian Andes (Argentina), Journal of Hydrology, 444-445, 134-145, https://doi.org/10.1016/j.jhydrol.2012.04.013, 2012.

Zhang, G., Bolch, T., Yao, T., Rounce, D. R., Chen, W., Veh, G., King, O., Allen, S. K., Wang, M., and Wang, W.: Underestimated mass loss from lake-terminating glaciers in the greater Himalaya, Nature Geoscience, 1-6, https://doi.org/10.1038/s41561-023-01150-1, 2023a.

Zhang, T., Wang, W., and An, B.: A massive lateral moraine collapse triggered the 2023 South Lhonak Lake outburst flood, Sikkim Himalayas, Landslides, 22, 299-311, 10.1007/s10346-024-02358-x, 2025.

Zhang, T., Wang, W., and An, B. J. T. C.: A conceptual model for glacial lake bathymetric distribution, 17, 5137-5154, 2023b.

Zhang, T., Wang, W., An, B., and Wei, L.: Enhanced glacial lake activity threatens numerous communities and infrastructure in the Third Pole, Nat Commun, 14, 8250, 10.1038/s41467-023-44123-z, 2023c.

Zhang, T., Wang, W., Gao, T., An, B., and Yao, T.: An integrative method for identifying potentially dangerous glacial lakes in the Himalayas, Sci Total Environ, 806, 150442, 10.1016/j.scitotenv.2021.150442, 2022.

Zheng, G., Mergili, M., Emmer, A., Allen, S., Bao, A., Guo, H., and Stoffel, M.: The 2020 glacial lake outburst flood at Jinwuco, Tibet: causes, impacts, and implications for hazard and risk assessment, The Cryosphere, 15, 3159-3180, 10.5194/tc-15-3159-2021, 2021a.

Zheng, G., Allen, S. K., Bao, A., Ballesteros-Cánovas, J. A., Huss, M., Zhang, G., Li, J., Yuan, Y., Jiang, L., Yu, T., Chen, W., and Stoffel, M.: Increasing risk of glacial lake outburst floods from future Third Pole deglaciation, Nature Climate Change, 11, 411-417, 10.1038/s41558-021-01028-3, 2021b.